California State Waters Map Series—Drakes Bay and Vicinity, California

By Janet T. Watt, Peter Dartnell, Nadine E. Golden, H. Gary Greene, Mercedes D. Erdey, Guy R. Cochrane, Samuel Y. Johnson, Stephen R. Hartwell, Rikk G. Kvitek, Michael W. Manson, Charles A. Endris, Bryan E. Dieter, Ray W. Sliter, Lisa M. Krigsman, Erik N. Lowe, and John L. Chin

(Janet T. Watt and Susan A. Cochran, editors)

Pamphlet to accompany

Open-File Report 2015–1041

2015

U.S. Department of the Interior
U.S. Geological Survey

U.S. Department of the Interior
SALLY JEWELL, Secretary

U.S. Geological Survey
Suzette M. Kimball, Acting Director

U.S. Geological Survey, Reston, Virginia: 2015

Suggested citation:
Watt, J.T., Dartnell, P., Golden, N.E., Greene, H.G., Erdey, M.D., Cochrane, G.R., Johnson, S.Y., Hartwell, S.R., Kvitek, R.G., Manson, M.W., Endris, C.A., Dieter, B.E., Sliter, R.W., Krigsman, L.M., Lowe, E.N., and Chin, J.L. (J.T. Watt and S.A. Cochran, eds.), 2015, California State Waters Map Series—Drakes Bay and Vicinity, California: U.S. Geological Survey Open-File Report 2015–1041, pamphlet 36 p., 10 sheets, scale 1:24,000, http://dx.doi.org/10.3133/ofr20151041.

ISSN 2331-1258 (online)

Contents

Figures

Tables

Map Sheets

California State Waters Map Series—Drakes Bay and Vicinity, California

By Janet T. Watt,[1] Peter Dartnell,[1] Nadine E. Golden,[1] H. Gary Greene,[2] Mercedes D. Erdey,[1] Guy R. Cochrane,[1] Samuel Y. Johnson,[1] Stephen R. Hartwell,[1] Rikk G. Kvitek,[3] Michael W. Manson,[4] Charles A. Endris,[2] Bryan E. Dieter,[2] Ray W. Sliter,[1] Lisa M. Krigsman,[5] Erik N. Lowe,[1] and John L. Chin[1]

(Janet T. Watt[1] and Susan A. Cochran,[1] editors)

Preface

In 2007, the California Ocean Protection Council initiated the California Seafloor Mapping Program (CSMP), designed to create a comprehensive seafloor map of high-resolution bathymetry, marine benthic habitats, and geology within California's State Waters. The program supports a large number of coastal-zone- and ocean-management issues, including the California Marine Life Protection Act (MLPA) (California Department of Fish and Wildlife, 2008), which requires information about the distribution of ecosystems as part of the design and proposal process for the establishment of Marine Protected Areas. A focus of CSMP is to map California's State Waters with consistent methods at a consistent scale.

The CSMP approach is to create highly detailed seafloor maps through collection, integration, interpretation, and visualization of swath sonar data (the undersea equivalent of satellite remote-sensing data in terrestrial mapping), acoustic backscatter, seafloor video, seafloor photography, high-resolution seismic-reflection profiles, and bottom-sediment sampling data. The map products display seafloor morphology and character, identify potential marine benthic habitats, and illustrate both the surficial seafloor geology and shallow (to about 100 m) subsurface geology. It is emphasized that the more interpretive habitat and geology maps rely on the integration of multiple, new high-resolution datasets and that mapping at small scales would not be possible without such data.

This approach and CSMP planning is based in part on recommendations of the Marine Mapping Planning Workshop (Kvitek and others, 2006), attended by coastal and marine managers and scientists from around the state. That workshop established geographic priorities for a coastal mapping project and identified the need for coverage of "lands" from the shore strand line (defined as Mean Higher High Water; MHHW) out to the 3-nautical-mile (5.6-km) limit of California's State Waters. Unfortunately, surveying the zone from MHHW out to 10-m water depth is not consistently possible using ship-based surveying methods, owing to sea state (for example, waves, wind, or currents), kelp coverage, and shallow rock outcrops. Accordingly, some of the maps presented in this series commonly do not cover the zone from the shore out to 10-m depth; these "no data" zones appear pale gray on most maps.

This map is part of a series of online U.S. Geological Survey (USGS) publications, each of which includes several map sheets, some explanatory text, and a descriptive pamphlet. Each map sheet

[1] U.S. Geological Survey
[2] Moss Landing Marine Laboratories, Center for Habitat Studies
[3] California State University, Monterey Bay, Seafloor Mapping Lab
[4] California Geological Survey
[5] National Oceanic and Atmospheric Administration, National Marine Fisheries Service

is published as a PDF file. Geographic information system (GIS) files that contain both ESRI[6] ArcGIS raster grids (for example, bathymetry, seafloor character) and geotiffs (for example, shaded relief) are also included for each publication. For those who do not own the full suite of ESRI GIS and mapping software, the data can be read using ESRI ArcReader, a free viewer that is available at http://www.esri.com/software/arcgis/arcreader/index.html (last accessed February 5, 2014).

The California Seafloor Mapping Program (CSMP) is a collaborative venture between numerous different federal and state agencies, academia, and the private sector. CSMP partners include the California Coastal Conservancy, the California Ocean Protection Council, the California Department of Fish and Wildlife, the California Geological Survey, California State University at Monterey Bay's Seafloor Mapping Lab, Moss Landing Marine Laboratories Center for Habitat Studies, Fugro Pelagos, Pacific Gas and Electric Company, National Oceanic and Atmospheric Administration (NOAA, including National Ocean Service – Office of Coast Surveys, National Marine Sanctuaries, and National Marine Fisheries Service), U.S. Army Corps of Engineers, the Bureau of Ocean Energy Management, the National Park Service, and the U.S. Geological Survey.

[6] Environmental Systems Research Institute, Inc.

Chapter 1. Introduction

By Janet T. Watt

Regional Setting

The map area offshore of Drakes Bay, California, which is referred to herein as the “Drakes Bay and Vicinity” map area (figs. 1–1, 1–2) is located in northern California, about 30 km north of San Francisco and about 65 km south of Fort Ross. The map area is in the northern part of the Gulf of the Farallones National Marine Sanctuary, and it includes all or parts of four California Marine Protected Areas (California Department of Fish and Wildlife, 2008): Point Reyes State Marine Reserve, Point Reyes Headlands Special Closure, Point Resistance Rock Special Closure, and Double Point/Stormy Stack Special Closure (fig. 1–2). The largely undeveloped onshore part of the map area, which occupies much of the southern and southeastern parts of the Point Reyes peninsula, is used primarily for grazing, as well as recreation, as it is home to the Point Reyes National Seashore. The triangular Point Reyes peninsula, which lies completely west of the San Andreas Fault Zone, is bounded by the steep terrain of Inverness Ridge along its northeastern margin, Tomales Point at its northernmost tip, Point Reyes at its southwesternmost point, and Bolinas at its southern end. The landscape in between includes (from southeast to northwest) the sandy beaches along Drakes Bay, the estuaries of Drakes Estero and Estero de Limantour, and the long, windswept Point Reyes Beach, which is backed by an extensive dune field (figs. 1–1, 1–2).

Tectonic influences that impact the shelf morphology and geology in the map area are related to local faulting, folding, uplift, and subsidence. Offshore of the Point Reyes headland, granitic basement rocks are offset vertically about 1.4 km along the Point Reyes Fault Zone (McCulloch, 1987); this uplift, combined with west-side-up offset on the San Andreas Fault Zone (Grove and Niemi, 2005), has resulted in uplift of the Point Reyes peninsula and the adjacent shelf (both the Bodega Head–Tomales Point shelf, north of the map area, and the Bolinas shelf; see sheet 9). Late Pleistocene uplift of marine terraces on the southern Point Reyes peninsula suggests active deformation of offshore structures west of the San Andreas Fault Zone (Grove and others, 2010). Pervasive stratal thinning within inferred uppermost Pliocene and Pleistocene (that is, post–Purisima Formation) deposits above the west strand of the Point Reyes Fault Zone suggests Quaternary active shortening of the curvilinear, northeast- to north-dipping Point Reyes Fault Zone. Lack of clear deformation in the uppermost Pleistocene and Holocene deposits suggests that activity along the Point Reyes Fault Zone has ceased or slowed since about 21,000 years ago. Although the cumulative (post-Miocene) slip rate on the Point Reyes Fault Zone in the map area is poorly constrained, it is estimated to be 0.3 mm/yr on the basis of vertical offset of granitic basement rocks (McCulloch, 1987; Wills and others, 2008).

The seafloor in the map area generally extends from the shoreline to water depths of about 40 to 50 m, except for the area south of the Point Reyes headland where water depths reach 60 to 70 m. This difference is the result of a distinct bathymetric gradient south and west of the Point Reyes headland, which is related to north-side-up motion along the Point Reyes Fault Zone (fig. 1–1). With the exception of the bathymetric gradient across the Point Reyes Fault Zone, the bedrock platform in the nearshore and inner shelf areas (50 to 60 m depth) is relatively flat (less than 1.0°) and is overlain by sand-sized to coarser grained sediment. Finer grained sediments are found in water depths greater than 60 m south of the Point Reyes headland, but they also extend into shallower (less than 40 m) water within Drakes Bay. Surficial and shallow sediments were deposited in the last about 21,000 years during the approximately 125-m sea-level rise that followed the last major lowstand associated with the Last Glacial Maximum (Fairbanks, 1989; Fleming and others, 1998; Lambeck and Chappell, 2001; Peltier and Fairbanks, 2006), at which time the entire Drakes Bay and Vicinity map area was emergent and the shoreline was about 30 km south and west of the present-day shoreline.

Potential marine benthic habitats in the Drakes Bay and Vicinity map area range from unconsolidated continental-shelf sediment to hard substrate, and they also include an anthropogenic feature (shipwreck). Rocky-shelf outcrops and rubble are considered to be promising potential habitats for rockfish and lingcod (Cass and others, 1990; Love and others, 2002), both of which are recreationally and commercially important species; in addition, the shipwreck might provide good potential habitat for rockfish.

Circulation over the continental shelf in the map area (and in the broader northern California region) is dominated by the southward-flowing California Current, the eastern limb of the North Pacific Gyre (Hickey, 1979). Associated upwelling brings cool, nutrient-rich waters to the surface, resulting in high biological productivity. The current flow generally is southeastward during the spring and summer; however, during the fall and winter, the otherwise persistent northwest winds are sometimes weak or absent, causing the California Current to move farther offshore and the Davidson Current, a weaker, northward-flowing countercurrent (Hickey, 1979), to become active.

Sediment transport in the map area largely is controlled by surface waves and tidal currents in the nearshore and, at depths greater than 20 to 30 m, by tidal and subtidal currents. In the map area, nearshore littoral drift of sand and coarse sediment is to the south (Patsch and Griggs, 2007), owing to the dominant west-northwest swell direction, and scour from large waves and tidal currents removes and redistributes sediment over large areas of the inner shelf. Tidal currents are particularly strong over the shelf in the Drakes Bay and Vicinity map area, and they dominate the current regime in the nearshore (Noble and Gelfenbaum, 1990; Noble, 2001). Further offshore, bottom currents generally flow to the northwest, distributing finer grained sediment accordingly (Noble and Gelfenbaum, 1990).

Publication Summary

This publication about the Drakes Bay and Vicinity map area includes ten map sheets that contain explanatory text, in addition to this descriptive pamphlet and a data catalog of geographic information system (GIS) files. Sheets 1, 2, and 3 combine data from four different sonar surveys to generate comprehensive high-resolution bathymetry and acoustic-backscatter coverage of the map area. These data reveal a range of physiographic features (highlighted in the perspective views on sheet 4) such as the flat, sediment-covered inner continental to midcontinental shelf, as well as shallow “scour depressions” and local, tectonically controlled bedrock uplifts. To validate geological and biological interpretations of the sonar data shown in sheets 1, 2, and 3, the U.S. Geological Survey towed a camera sled over specific offshore locations, collecting both video and photographic imagery; these “ground-truth” surveying data are summarized on sheet 6. Sheet 5 is a “seafloor character” map, which classifies the seafloor on the basis of depth, slope, rugosity (ruggedness), and backscatter intensity and which is further informed by the ground-truth-survey imagery. Sheet 7 is a map of “potential habitats,” which are delineated on the basis of substrate type, geomorphology, seafloor process, or other attributes that may provide a habitat for a specific species or assemblage of organisms. Sheet 8 compiles representative seismic-reflection profiles from the map area, providing information on the subsurface stratigraphy and structure of the map area. Sheet 9 shows the distribution and thickness of young sediment (deposited over the last about 21,000 years, during the most recent sea-level rise) in both the map area and the larger Salt Point to Drakes Bay region, interpreted on the basis of the seismic-reflection data, and it identifies the Drakes Bay and Vicinity map area as lying within the Point Reyes bar and Bolinas shelf domains. Sheet 10 is a geologic map that merges onshore geologic mapping (compiled from existing maps by the California Geological Survey) and new offshore geologic mapping that is based on integration of high-resolution bathymetry and backscatter imagery (sheets 1, 2, 3), seafloor-sediment and rock samples (Reid and others, 2006), digital camera and video imagery (sheet 6), and high-resolution seismic-reflection profiles (sheet 8).

The information provided by the map sheets, pamphlet, and data catalog have a broad range of applications. High-resolution bathymetry, acoustic backscatter, ground-truth-surveying imagery, and habitat mapping all contribute to habitat characterization and ecosystem-based management by providing essential data for delineation of marine protected areas and ecosystem restoration. Many of the maps provide high-resolution baselines that will be critical for monitoring environmental change

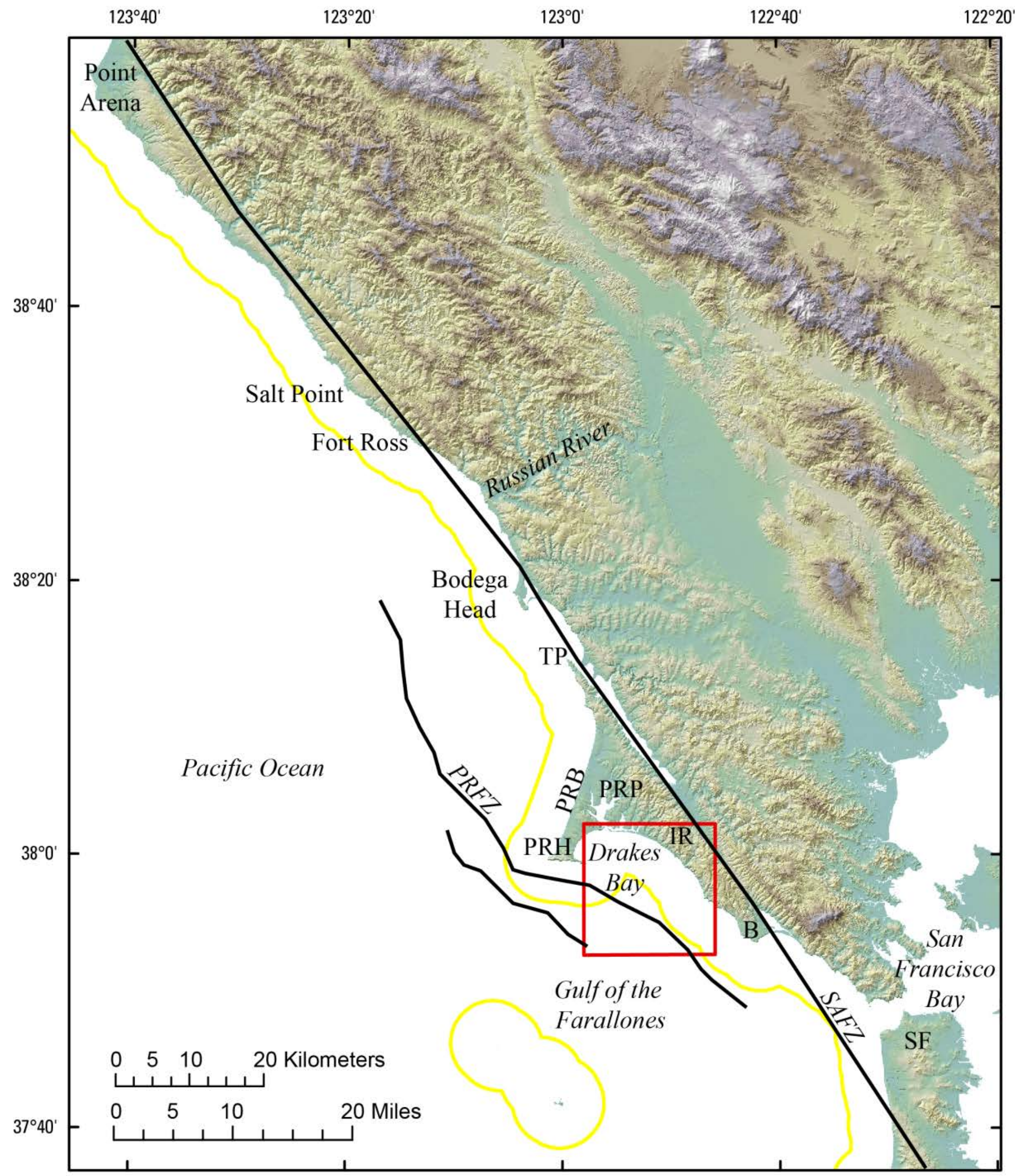

Figure 1–1. Physiography of northern California coast from Point Arena to San Francisco (SF). Red box shows Drakes Bay and Vicinity map area. Yellow line shows limit of California's State Waters. Black lines show faults (PRFZ, Point Reyes Fault Zone; SAFZ, San Andreas Fault Zone). Other abbreviations: B, Bolinas; IR, Inverness Ridge; PRB, Point Reyes Beach; PRH, Point Reyes headland; PRP, Point Reyes peninsula; SF, San Francisco; TP, Tomales Point.

associated with climate change, coastal development, or other forcings. High-resolution bathymetry is a critical component for modeling coastal flooding caused by storms and tsunamis, as well as inundation associated with longer term sea-level rise. Seismic-reflection and bathymetric data help characterize earthquake and tsunami sources, critical for natural-hazard assessments of coastal zones. Information on sediment distribution and thickness is essential to the understanding of local and regional sediment transport, as well as the development of regional sediment-management plans. In addition, siting of any new offshore infrastructure (for example, pipelines, cables, or renewable-energy facilities) will depend on high-resolution mapping. Finally, this mapping will both stimulate and enable new scientific research and also raise public awareness of, and education about, coastal environments and issues.

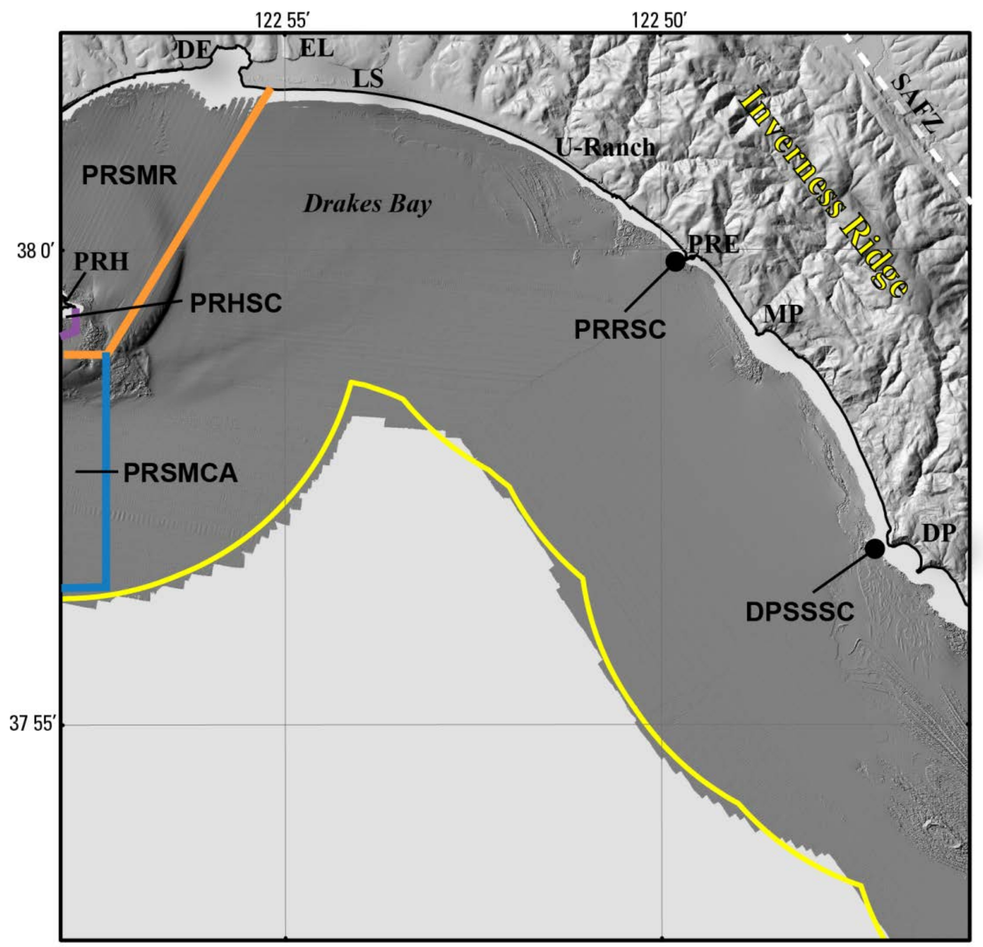

Figure 1–2. Coastal geography of Drakes Bay and Vicinity map area. Yellow line shows limit of California's State Waters. Dashed white line shows trace of San Andreas Fault Zone (SAFZ). Indicated on map are California Marine Protected Areas: DPSSSC, Double Point/Stormy Stack Special Closure; PRHSC, Point Reyes Headlands Special Closure (purple outline); PRRSC, Point Resistance Rock Special Closure; PRSMCA, Point Reyes State Marine Conservation Area (blue outline); PRSMR, Point Reyes State Marine Reserve (orange outline). Other abbreviations: DE, Drakes Estero; DP, Double Point; EL, Estero de Limantour; LS, Limantour Spit; MP, Millers Point; PRE, Point Resistance; PRH, Point Reyes headland.

Chapter 2. Bathymetry and Backscatter-Intensity Maps of the Drakes Bay and Vicinity Map Area (Sheets 1, 2, and 3)

By Peter Dartnell and Rikk G. Kvitek

The colored shaded-relief bathymetry (sheet 1), the shaded-relief bathymetry (sheet 2), and the acoustic-backscatter (sheet 3) maps of the Drakes Bay and Vicinity map area in northern California were generated from bathymetry and backscatter data collected by Fugro Pelagos and by California State University, Monterey Bay (CSUMB) (fig. 1 on sheets 1, 2, 3). Mapping was completed between 2007 and 2010, using a combination of 200-kHz and 400-kHz Reson 7125 and 244-kHz Reson 8101 multibeam echosounders, as well as a 468-kHz SEA SWATHplus bathymetric sidescan-sonar system. These mapping missions combined to collect both bathymetry (sheets 1, 2) and acoustic-backscatter data (sheet 3) from about the 10-m isobath to beyond the 3-nautical-mile limit of California's State Waters.

During the mapping missions, an Applanix POS MV (Position and Orientation System for Marine Vessels) was used to accurately position the vessels during data collection, and it also accounted for vessel motion such as heave, pitch, and roll (position accuracy, ±2 m; pitch, roll, and heading accuracy, ±0.02°; heave accuracy, ±5%, or 5 cm). To account for tidal-cycle fluctuations, CSUMB used NavCom 2050 GPS receiver (CNAV) data, and Fugro Pelagos used KGPS data (GPS data with real-time kinematic corrections); in addition, sound-velocity profiles were collected with an Applied Microsystems (AM) SVPlus sound velocimeter. Soundings were corrected for vessel motion using the Applanix POS MV data, for variations in water-column sound velocity using the AM SVPlus data, and for variations in water height (tides) using vertical-position data from the KGPS receivers.

The multibeam-echosounder backscatter data were postprocessed using CARIS 7.0/Geocoder software. Within Geocoder, the backscatter intensities were radiometrically corrected (including despeckling and angle-varying gain adjustments), and the position of each acoustic sample was geometrically corrected for slant range on a line-by-line basis. After the lines were corrected, they were mosaicked into a 1-m-resolution image. Overlap between parallel lines was resolved using a priority table whose values were based on the distance of each sample from the ship track, with the samples that were closest to and furthest from the ship track being given the lowest priority. An anti-aliasing algorithm was also applied. The mosaics were then exported as georeferenced TIFF images, imported into a geographic information system (GIS), and converted to GRIDs at 2-m resolution.

The SWATHplus backscatter data were postprocessed using USGS software (D.P. Finlayson, written commun., 2011) that normalizes for time-varying signal loss and beam-directivity differences. Thus, the raw 16-bit backscatter data were gain-normalized to enhance the backscatter of the SWATHplus system. The resulting normalized-amplitude values were rescaled to 16-bit and gridded into GeoJPEGs using GRID Processor Software, then imported into a GIS and converted to GRIDs.

Processed soundings from the different mapping missions were exported from the acquisition or processing software as XYZ files and bathymetric surfaces. All the surfaces were merged into one overall 2-m-resolution bathymetric-surface model and clipped to the boundary of the map area. An illumination having an azimuth of 300° and from 45° above the horizon was then applied to the bathymetric surface to create the shaded-relief imagery (sheets 1, 2). In addition, a modified "rainbow" color ramp was applied to the bathymetry data for sheet 1, using reds and oranges to represent shallower depths, and blues to represent greater depths (note that the Drakes Bay and Vicinity map area requires only the shallower part of the full-rainbow color ramp used on some of the other maps in the California State Waters Map Series; see, for example, Kvitek and others, 2012). This colored bathymetry surface was draped over the shaded-relief imagery at 60-percent transparency to create a colored shaded-relief map (sheet 1). Note that the ripple patterns and straight lines that are apparent within the map area are data-collection artifacts. In addition, lines at the borders of some surveys are the result of slight differences in depth, as measured by different mapping systems in different years. These various artifacts are made obvious by the hillshading process.

Bathymetric contours (sheets 1, 2, 3, 5, 7, 10) were generated at 10-m intervals from the merged 2-m-resolution bathymetric surface. The most continuous contour segments were preserved; smaller segments and isolated island polygons were excluded from the final output. Contours were smoothed using a polynomial approximation with exponential kernel algorithm and a tolerance value of 60 m.

The acoustic-backscatter imagery from each different mapping system and processing method were merged into their own individual grids. These individual grids, which cover different areas, were displayed in a GIS to create an acoustic-backscatter map (sheet 3). On the map, brighter tones indicate higher backscatter intensity, and darker tones indicate lower backscatter intensity. The intensity represents a complex interaction between the acoustic pulse and the seafloor, as well as characteristics within the shallow subsurface, providing a general indication of seafloor texture and sediment type. Backscatter intensity depends on the acoustic source level; the frequency used to image the seafloor; the grazing angle; the composition and character of the seafloor, including grain size, water content, bulk density, and seafloor roughness; and some biological cover. Harder and rougher bottom types such as rocky outcrops or coarse sediment typically return stronger intensities (high backscatter, lighter tones), whereas softer bottom types such as fine sediment return weaker intensities (low backscatter, darker tones).

The onshore-area image was generated by applying an illumination having an azimuth of 300° and from 45° above the horizon to 3-m-resolution topographic-lidar data from the U.S. Geological Survey's National Elevation Dataset (available at http://ned.usgs.gov/).

Chapter 3. Data Integration and Visualization for the Drakes Bay and Vicinity Map Area (Sheet 4)

By Peter Dartnell

Mapping California's State Waters has produced a vast amount of acoustic and visual data, including bathymetry, acoustic backscatter, seismic-reflection profiles, and seafloor video and photography. These data are used by researchers to develop maps, reports, and other tools to assist in the coastal and marine spatial-planning capability of coastal-zone managers and other stakeholders. For example, seafloor-character (sheet 5), habitat (sheet 7), and geologic (sheet 10) maps of the Drakes Bay and Vicinity map area may assist in the designation of Marine Protected Areas, as well as in their monitoring. These maps and reports also help to analyze environmental change owing to sea-level rise and coastal development, to model and predict sediment and contaminant budgets and transport, to site offshore infrastructure, and to assess tsunami and earthquake hazards. To facilitate this increased understanding and to assist in product development, it is helpful to integrate the different datasets and then view the results in three-dimensional representations such as those displayed on the data integration and visualization sheet for the Drakes Bay and Vicinity map area (sheet 4).

The maps and three-dimensional views on sheet 4 were created using a series of geographic information systems (GIS) and visualization techniques. Using GIS, the bathymetric and topographic data (sheet 1) were converted to ASCIIRASTER format files, and the acoustic-backscatter data (sheet 3) were converted to geoTIFF images. The bathymetric and topographic data were imported in the Fledermaus® software (QPS). The bathymetry was color-coded to closely match the colored shaded-relief bathymetry on sheet 1 in which reds and oranges represent shallower depths and greens represent deeper depths. Topographic data were shown in gray shades. The acoustic-backscatter geoTIFF images were also draped over the bathymetry data. The colored bathymetry, topography, and draped backscatter were then tilted and panned to create the perspective views such as those shown in figures 1 through 6 on sheet 4. These figures highlight the seafloor morphology in the Drakes Bay and Vicinity map area, which includes outcrops of fractured bedrock and complex patterns of shallow depressions.

Block diagrams that combine the bathymetry with seismic-reflection-profile data help integrate surface and subsurface observations, especially stratigraphic and structural relations (for example, fig. 6 on sheet 4). These block diagrams were created by converting digital seismic-reflection-profile data (see sheet 8) into TIFF images, while taking note of the starting and ending coordinates and maximum and minimum depths. The images were then imported into the Fledermaus® software as vertical images and merged with the bathymetry imagery.

Chapter 4. Seafloor-Character Map of the Drakes Bay and Vicinity Map Area (Sheet 5)

By Mercedes D. Erdey and Guy R. Cochrane

The California State Marine Life Protection Act (MLPA) calls for protecting representative types of habitat in different depth zones and environmental conditions. A science team, assembled under the auspices of the California Department of Fish and Wildlife (CDFW), has identified seven substrate-defined seafloor habitats in California's State Waters that can be classified using sonar data and seafloor video and photography. These habitats include rocky banks, intertidal zones, sandy or soft ocean bottoms, underwater pinnacles, kelp forests, submarine canyons, and seagrass beds. The following five depth zones, which determine changes in species composition, have been identified: Depth Zone 1, intertidal; Depth Zone 2, intertidal to 30 m; Depth Zone 3, 30 to 100 m; Depth Zone 4, 100 to 200 m; and Depth Zone 5, deeper than 200 m (California Department of Fish and Wildlife, 2008). The CDFW habitats, with the exception of depth zones, can be considered a subset of a broader classification scheme of Greene and others (1999) that has been used by the U.S. Geological Survey (USGS) (Cochrane and others, 2003, 2005). These seafloor-character maps are generalized polygon shapefiles that have attributes derived from Greene and others (2007).

A 2007 Coastal Map Development Workshop, hosted by the USGS in Menlo Park, California, identified the need for more detailed (relative to Greene and others' [1999] attributes) raster products that preserve some of the transitional character of the seafloor when substrates are mixed and (or) they change gradationally. The seafloor-character map, which delineates a subset of the CDFW habitats, is a GIS-derived raster product that can be produced in a consistent manner from data of variable quality covering large geographic regions.

The following four substrate classes are identified in the Drakes Bay and Vicinity map area:

- Class I: Fine- to medium-grained smooth sediment
- Class II: Mixed smooth sediment and rock
- Class III: Rock and boulder, rugose
- Class IV: Medium- to coarse-grained sediment (in scour depressions)

The seafloor-character map of the Drakes Bay and Vicinity map area (sheet 5) was produced using video-supervised maximum-likelihood classification of the bathymetry and intensity of return from sonar systems, following the method described by Cochrane (2008). The two variants used in this classification were backscatter intensity and derivative rugosity. Rugosity calculation was performed using the Terrain Ruggedness (VRM) tool within the Benthic Terrain Modeler toolset v. 3.0 (Wright and others, 2012; available at http://esriurl.com/5754).

Classes I, II, and III values were delineated using multivariate analysis. Class IV (medium- to coarse-grained sediment, in scour depressions) values were determined on the basis of their visual characteristics using both shaded-relief bathymetry and backscatter (slight depression in the seafloor, very high backscatter return). The resulting map (gridded at 2 m) was cleaned by hand to remove data collection artifacts (for example, the trackline nadir).

On the seafloor-character map (sheet 5), the four substrate classes have been colored to indicate the California MLPA depth zones and the Coastal and Marine Ecological Classification Standard (CMECS) slope zones (Madden and others, 2008) in which they belong. The California MLPA depth zones are Depth Zone 1 (intertidal), Depth Zone 2 (intertidal to 30 m), Depth Zone 3 (30 to 100 m), Depth Zone 4 (100 to 200 m), and Depth Zone 5 (greater than 200 m); in the Drakes Bay and Vicinity map area, only Depth Zones 2 and 3 are present. The slope classes that represent the CMECS slope zones are Slope Class 1 = flat (0° to 5°), Slope Class 2 = sloping (5° to 30°), Slope Class 3 = steeply sloping (30° to 60°), Slope Class 4 = vertical (60° to 90°), and Slope Class 5 = overhang (greater than 90°); in the Drakes Bay and Vicinity map area, only Slope Classes 1 and 2 are present. The final classified seafloor-character raster map image has been draped over the shaded-relief bathymetry for the area (sheets 1 and 2) to produce the image shown on the seafloor-character map on sheet 5.

The seafloor-character classification also is summarized on sheet 5 in table 1. Fine- to medium-grained smooth sediment (sand and mud) makes up 87.8 percent (127.5 km^2) of the map area: 24.6 percent (35.7 km^2) is in Depth Zone 2, and 63.2 percent (91.8 km^2) is in Depth Zone 3. Mixed smooth sediment (sand and gravel) and rock (that is, sediment typically forming a veneer over bedrock, or rock outcrops having little to no relief) make up 6.3 percent (9.2 km^2) of the map area: 4.8 percent (7.0 km^2) is in Depth Zone 2, and 1.5 percent (2.2 km^2) is in Depth Zone 3. Rock and boulder, rugose (rock and boulder outcrops having high surficial complexity) makes up 2.6 percent (3.7 km^2) of the map area: 2.3 percent (3.3 km^2) is in Depth Zone 2, and 0.3 percent (0.4 km^2) is in Depth Zone 3. Medium- to coarse-grained sediment (in scour depressions consisting of material that is coarser than the surrounding seafloor) makes up 3.4 percent (4.9 km^2) of the map area: 2.9 percent (4.2 km^2) is in Depth Zone 2, and 0.5 percent (0.7 km^2) is in Depth Zone 3.

A small number of video observations were used to supervise the numerical classification of the seafloor. All video observations (see sheet 6) are used for accuracy assessment of the seafloor-character map after classification. To compare observations to classified pixels, each observation point is assigned a class (I, II, or III), according to the visually derived, major or minor geologic component (for example, sand or rock) and the abiotic complexity (vertical variability) of the substrate recorded during ground-truth surveys (table 4–1; see also, chapter 5 of this pamphlet). Class IV values were assigned on the basis of the observation of one or more of a group of features that includes both larger scale bedforms (for example, sand waves), as well as sediment-filled scour depressions that resemble the “rippled scour depressions” of Cacchione and others (1984) and Phillips and others (2007) and also the “sorted bedforms” of Murray and Thieler (2004), Goff and others (2005), and Trembanis and Hume (2011). On the geologic map (see sheet 10 of this report), they are referred to as “marine shelf scour depressions.”

Next, circular buffer areas were created around individual observation points using a 10-m radius to account for layback and positional inaccuracies inherent to the towed-camera system. The radius length is an average of the distances between the positions of sharp interfaces seen on both the video (the position of the ship at the time of observation) and sonar data, plus the distance covered during a 10-second observation period at an average speed of 1 nautical mile/hour. Each buffer, which covers more than 300 m^2, contains approximately 77 pixels. The classified (I, II, III) buffer is used as a mask to extract pixels from the seafloor-character map. These pixels are then compared to the class of the buffer. For example, if the shipboard-video observation is Class II (mixed smooth sediment and rock), but 12 of the 77 pixels within the buffer area are characterized as Class I (fine- to medium-grained smooth sediment), and 15 (of the 77) are characterized as Class III (rock and boulder, rugose), then the comparison would be “Class I, 12; Class II, 50; Class III, 15” (fig. 4–1). If the video observation of substrate is Class II, then the classification is accurate because the majority of seafloor pixels in the buffer are Class II. The accuracy values in table 4–2 represent the final of several classification iterations aimed at achieving the best accuracy, given the variable quality of sonar data (see discussion in Cochrane, 2008) and the limited ground-truth information available when compared to the continuous coverage provided by swath sonar. Presence/absence values in table 4–2 reflect the percentages of observations where the sediment classification of at least one pixel within the buffer zone agreed with the observed sediment type at a certain location.

The seafloor in the Drakes Bay and Vicinity map area is covered predominantly by Class I sediment composed of sand and mud. Several small exposures of rugose bedrock (Class III) are present in the nearshore area, and a larger area of fractured and folded bedrock outcrop dominates the southeastern part of the map area. The rock outcrops are covered with varying thicknesses of fine (Class I) to coarse (Class II) sediment. Several areas of medium- to coarse-grained scour depressions (Class IV) also have been identified adjacent to rock outcrops.

The classification accuracy of Class I (75 percent accurate; table 4–2) is determined by comparing the shipboard video observations and the classified map. The weaker agreements in Classes II and III (40 percent and 17 percent accurate, respectively) likely are due to the relatively narrow and intermittent nature of transition zones from sediment to rock and also the size of the buffer. The bedrock outcrops in this area are composed of differentially eroded sedimentary rocks (Cochrane and Lafferty, 2002). Erosion of softer layers produces Class I and II sediments, resulting in patchy areas of rugose rock and boulder habitat (Class III) on the seafloor. A single buffered observation locale of 78 pixels, therefore, is likely to be interspersed with other classes of pixels, in addition to Class III. Percentages for presence/absence within a buffer also were calculated as a better measure of the accuracy of the classification for patchy rock habitat. The presence/absence accuracy was found to be significant for Classes I, II, and III (91 percent significant, 93 percent significant, and 52 percent significant, respectively). No video observations were retrieved over Class IV substrate (medium- to coarse grained sediment); therefore, no accuracy assessments were performed for this class.

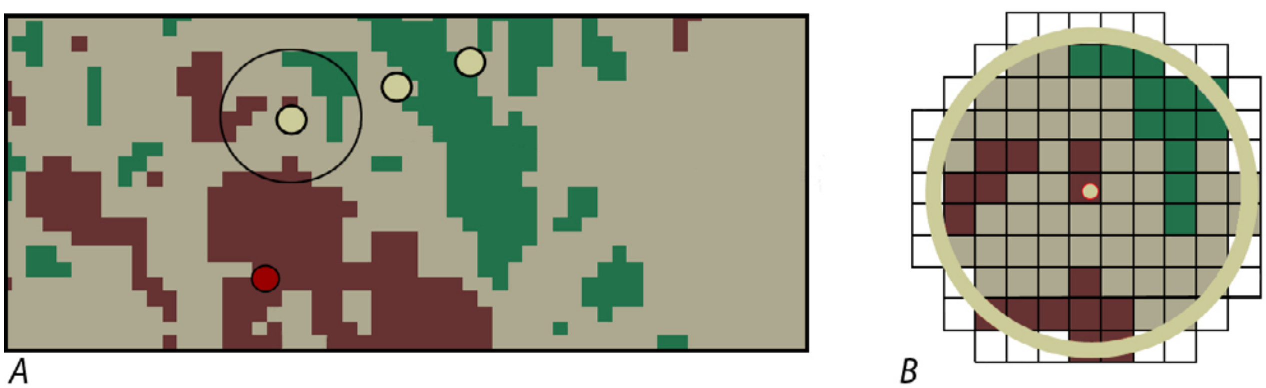

Figure 4–1. Detailed view of ground-truth data, showing accuracy-assessment methodology. *A*, Dots illustrate ground-truth observation points, each of which represents 10-second window of substrate observation plotted over seafloor-character grid; circle around dot illustrates area of buffer depicted in *B*. *B*, Pixels of seafloor-character data within 10-m-radius buffer centered on one individual ground-truth video observation.

Table 4–1. Conversion table showing how video observations of primary substrate (more than 50 percent seafloor coverage), secondary substrate (more than 20 percent seafloor coverage), and abiotic seafloor complexity (in first three columns) are grouped into seafloor-character-map Classes I, II, and III for use in supervised classification and accuracy assessment in Drakes Bay and Vicinity map area.

[In areas of low visibility where primary and secondary substrate could not be identified with confidence, recorded observations of substrate (in fourth column) were used to assess accuracy]

Primary-substrate component	Secondary-substrate component	Abiotic seafloor complexity	Low-visibility observations
Class I			
mud	sand	low	
mud	sand	moderate	
sand	mud	low	
sand	mud	moderate	
sand	sand	low	
sand	sand	moderate	
			sediment
			mud component
			ripples
Class II			
cobbles	cobbles	low	
cobbles	mud	low	
cobbles	sand	low	
sand	cobbles	low	
sand	cobbles	moderate	
sand	gravel	low	
Class III			
boulders	boulders	moderate	
boulders	cobbles	moderate	
boulders	rock	moderate	
boulders	sand	moderate	
sand	boulders	moderate	
sand	rock	moderate	
rock	boulders	moderate	
rock	cobbles	high	
rock	cobbles	moderate	
rock	rock	low	
rock	rock	moderate	
rock	rock	high	
rock	sand	moderate	

Table 4–2. Accuracy-assessment statistics for seafloor-character-map classifications in Drakes Bay and Vicinity map area.

[Accuracy assessments are based on video observations (N/A, no accuracy assessment was conducted)]

Class	Number of observations	% majority	% presence/absence
I—Fine- to medium-grained smooth sediment	194	75.0	90.7
II—Mixed smooth sediment and rock	27	39.7	92.6
III—Rock and boulder, rugose	63	17.4	52.4
IV— Medium- to coarse-grained sediment (in scour depressions	0	N/A	N/A

Chapter 5. Ground-Truth Studies for the Drakes Bay and Vicinity Map Area (Sheet 6)

By Nadine E. Golden and Guy R. Cochrane

To validate the interpretations of sonar data in order to turn it into geologically and biologically useful information, the U.S. Geological Survey (USGS) towed a camera sled (fig. 5–1) over specific locations throughout the Drakes Bay and Vicinity map area to collect video and photographic data that would "ground truth" the seafloor. This ground-truth surveying occurred in 2007. The camera sled was towed 1 to 2 m above the seafloor at speeds of between 1 and 2 nautical miles/hour. Ground-truth surveys in this map area include approximately 6 trackline kilometers of video and 770 still photographs, in addition to 742 recorded seafloor observations of abiotic and biotic attributes. A visual estimate of slope also was recorded.

During the cruise, the USGS camera sled housed two standard-definition (640×480 pixel resolution) video cameras (one forward looking and one downward looking), a high-definition (1,080×1,920 pixel resolution) video camera, and an 8-megapixel digital still camera. During this cruise, in addition to recording the seafloor characteristics, a digital still photograph was captured once every 30 seconds.

The camera-sled tracklines (shown by colored dots on the map on sheet 6) are sited in order to visually inspect areas representative of the full range of bottom hardness and rugosity in the map area. The video is fed in real time to the research vessel, where USGS and National Oceanic and Atmospheric Administration (NOAA) scientists record both the geologic and biologic character of the seafloor. While the camera is deployed, several different observations are recorded for a 10-second period once every minute, using the protocol of Anderson and others (2007). Observations of primary substrate, secondary

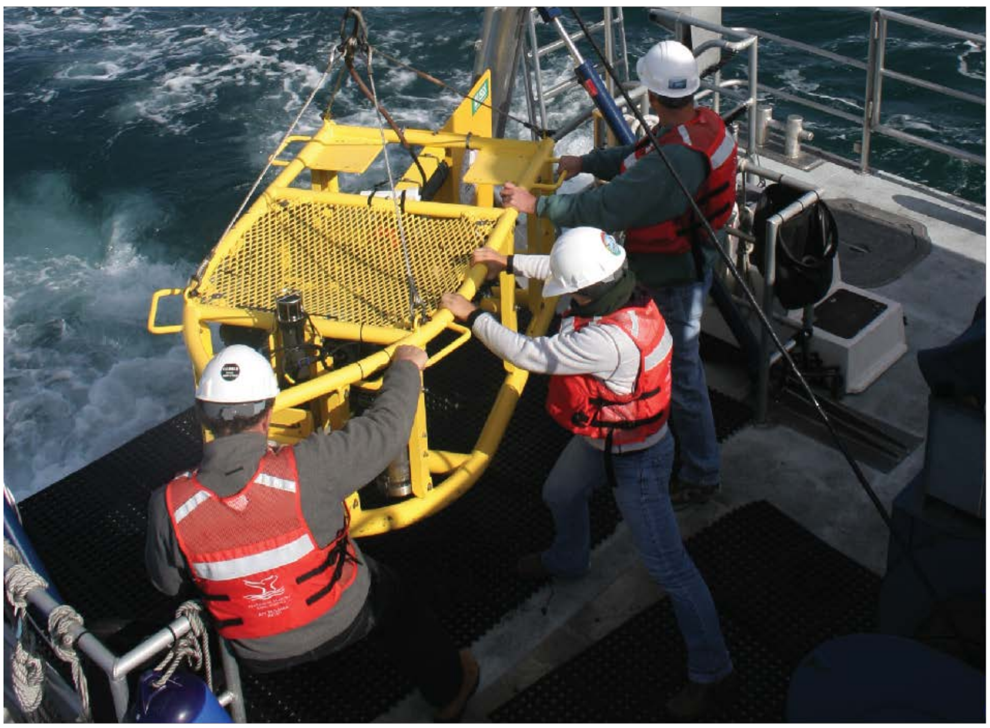

Figure 5–1. Photograph of camera sled used in USGS 2007 ground-truth survey.

substrate, slope, abiotic complexity, biotic complexity, and biotic cover are mandatory. Observations of key geologic features and the presence of key species also are made.

Primary and secondary substrate, by definition, constitute greater than 50 and 20 percent of the seafloor, respectively, during an observation. The grain-size values that differentiate the substrate classes are based on the Wentworth (1922) scale, and the sand, cobble, and boulder sizes are classified as in Wentworth (1922). However, the difficulty in distinguishing the finest divisions in the Wentworth (1922) scale during video observations made it necessary to aggregate some grain-size classes, as was done in the Anderson and others (2007) methodology: the granule and pebble sizes have been grouped together into a class called “gravel,” and the clay and silt sizes have been grouped together into a class called “mud.” In addition, hard bottom and clasts larger than boulder size are classified as “rock.” Benthic-habitat complexity, which is divided into abiotic (geologic) and biotic (biologic) components, refers to the visual classification of local geologic features and biota that potentially can provide refuge for both juvenile and adult forms of various species (Tissot and others, 2006).

Sheet 6 contains a smaller, simplified (depth-zone symbology has been removed) version of the seafloor-character map on sheet 5. On this simplified map, the camera-sled tracklines used to ground-truth-survey the sonar data are shown by aligned colored dots, each dot representing the location of a recorded observation. A combination of abiotic attributes (primary- and secondary-substrate compositions), as well as vertical variability, were used to derive the different classes represented on the seafloor-character map (sheet 5); on the simplified map, the derived classes are represented by colored dots. Also on this map are locations of the detailed views of seafloor character, shown by boxes (Boxes A through C); for each view, the box shows the locations (indicated by colored stars) of representative seafloor photographs. For each photograph, an explanation of the observed seafloor characteristics recorded by USGS and NOAA scientists is given. Note that individual photographs often show more substrate types than are reported as the primary and secondary substrate. Organisms, when present, are labeled on the photographs.

The ground-truth survey is designed to investigate areas that represent the full spectrum of high-resolution multibeam bathymetry and backscatter-intensity variation. Figure 5–2 shows that, in the Drakes Bay and Vicinity map area, the seafloor surface is predominantly fine-grained sandy sediment (see also, figs. 1B, 3C on sheet 6) in the relatively sheltered Drakes Bay. Muddy sediments likely are found in deeper water on the basis of ground-truth surveys north and south of the map area. Massive plutonic rocks form rocky outcrops in wave-exposed nearshore areas along the coast southeast of the Point Reyes headland (see also, sheet 10). In the east half of the map area, areas of rocky outcrop composed of layered sedimentary rocks (see fig. 3D on sheet 6) extend into deeper water.

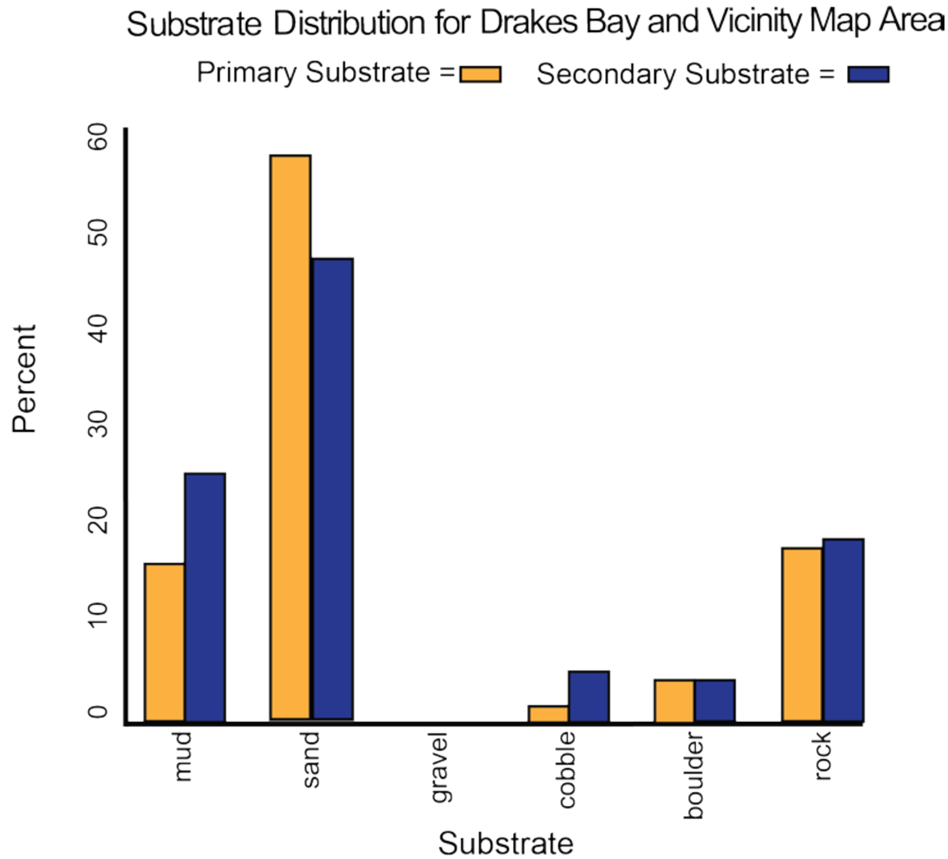

Figure 5–2. Graph showing distribution of primary and secondary substrate determined from video observations in Drakes Bay and Vicinity map area.

Chapter 6. Potential Marine Benthic Habitats of the Drakes Bay and Vicinity Map Area (Sheet 7)

By H. Gary Greene, Charles A. Endris, and Bryan E. Dieter

The map on sheet 7 shows “potential” marine benthic habitats in the Drakes Bay and Vicinity map area, representing a substrate type, geomorphology, seafloor process, or any other attribute that may provide a habitat for a specific species or assemblage of organisms. This map, which is based largely on seafloor geology, also integrates information displayed on several other thematic maps of the Drakes Bay and Vicinity map area. High-resolution sonar bathymetry data, converted to depth grids (seafloor DEMs; sheet 1), are essential to development of the potential marine benthic habitat map, as is shaded-relief imagery (sheet 2), which allows visualization of seafloor terrain and provides a foundation for interpretation of submarine landforms.

Backscatter maps (sheet 3) also are essential for developing potential benthic habitat maps. High backscatter is further indication of “hard” bottom, consistent with interpretation as rock or coarse sediment. Low backscatter, indicative of a “soft” bottom, generally indicates a fine-sediment environment. Habitat interpretations also are informed by actual seafloor observations from ground-truth surveying (sheet 6), by seafloor-character maps that are based on video-supervised maximum-likelihood classification (sheet 5), and by seafloor-geology maps (sheet 10). The habitat interpretations on sheet 7 are further informed by the usSEABED bottom-sampling compilation of Reid and others (2006).

Broad, generally smooth areas of seafloor that lack sharp and angular edge characteristics are mapped as “sediment;” these areas may be further defined by various sedimentary features (for example, erosional scours and depressions) and (or) depositional features (for example, dunes, mounds, or sand waves). In contrast, many areas of seafloor bedrock exposures are identified by their common sharp edges and high relative relief; these may be contiguous outcrops, isolated parts of outcrop protruding through sediment cover (pinnacles or knobs), or isolated boulders. In many locations, areas within or around a rocky feature appear to be covered by a thin veneer of sediment; these areas are identified on the habitat map as “mixed” induration (that is, containing both rock and sediment). The combination of remotely observed data (for example, high-resolution bathymetry and backscatter, seismic-reflection profiles) and directly observed data (for example, camera transects, sediment samples) translates to higher confidence in the ability to interpret broad areas of the seafloor.

To avoid any possible misunderstanding of the term “habitat,” the term “potential habitat” (as defined by Greene and others, 2005) is used herein to describe a set of distinct seafloor conditions that in the future may qualify as an “actual habitat.” Once habitat associations of a species are determined, they can be used to create maps that depict actual habitats, which then need to be confirmed by in situ observations, video, and (or) photographic documentation.

Classifying Potential Marine Benthic Habitats

Potential marine benthic habitats in the Drakes Bay and Vicinity map area are mapped using the Benthic Marine Potential Habitat Classification Scheme, a mapping-attribute code developed by Greene and others (1999, 2007). This code, which has been used previously in other offshore California areas (see, for example, Greene and others, 2005, 2007), was developed to easily create categories of marine benthic habitats that can then be queried within a GIS or a database. The code contains several categories that can be subdivided relative to the spatial scale of the data. The following categories can be applied directly to habitat interpretations determined from remote-sensing imagery collected at a scale of tens of kilometers to one meter: Megahabitat, Seafloor Induration, Meso/Macrohabitat, Modifier, Seafloor Slope, Seafloor Complexity, and Geologic Unit. Additional categories of Macro/Microhabitat, Seafloor Slope, Seafloor Complexity, and Geologic Attribute can be applied to habitat interpretations determined from seafloor samples, video, still photographs, or direct observations at a scale of 10 meters to a few centimeters. These two scale-dependent groups of categories can be used together, to define a habitat across spatial scales, or separately, to compare large- and small-scale habitat types.

The four categories and their attribute codes that are used on the Drakes Bay and Vicinity map are explained in detail below (note, however, that not all categories may be used in a particular map area, given the study objectives, data availability, or data quality); attribute codes in each category are depicted on the map by the letters and, in some cases, numbers that make up the map-unit symbols:

Megahabitat—Based on depth and general physiographic boundaries; used to distinguish features on a scale of tens of kilometers to kilometers. Depicted on map by capital letter, listed first in map-unit symbol; generalized depth ranges are given below.

E = Estuary (0 to 100 m)
S = Shelf; continental and island shelves (0 to 200 m)

Seafloor Induration—Refers to substrate hardness. Depicted on map by lower-case letter, listed second in map-unit symbol; may be further subdivided into distinct sediment types, depicted by lower-case letter(s) in parentheses, listed immediately after substrate hardness; multiple attributes listed in general order of relative abundance, separated by slash; queried where inferred.

h = Hard bottom (for example, rock outcrop or sediment pavement)
m = Mixed hard and soft bottom (for example, local sediment cover of bedrock)
s = Soft bottom; sediment cover
(b) = Boulders
(g) = Gravel
(s) = Sand
(m) = Mud, silt, and (or) clay

Meso/Macrohabitat—Related to scale of habitat; consists of seafloor features one kilometer to one meter in size. Depicted on map by lower-case letter and, in some cases, additional lower-case letter in parentheses, listed third in map-unit symbol; multiple attributes separated by slash.

b = Beach, relic (submerged) or shoreline
(b)/p = Pinnacle indistinguishable from boulder
d = Deformed, tilted and (or) folded bedrock; overhang
e = Exposure; bedrock
h = Hole; depression
m = Mound; linear ridge
p = Pinnacle; cone
s = Scarp, cliff, fault, or slump scar
w = Dynamic bedform
y = Delta; fan

Modifier—Describes texture, bedforms, biology, or lithology of seafloor. Depicted on map by lower-case letter, in some cases followed by additional lower-case letter(s) either after hyphen or in parentheses (or both), following an underscore; multiple attributes separated by slash.

_a = Anthropogenic (artificial reef, breakwall, shipwreck, disturbance)
  _a-dg = Dredge groove or channel
  _a-g = Groin, jetty, rip-rap
  _a-w = Wreck, ship, barge, or plane
_c = Consolidated sediment (claystone, mudstone, siltstone, sandstone, breccia, or conglomerate)
_d = Differentially eroded
_f = Fracture, joint; faulted

_g = Granite
_h = Hummocky, irregular relief
_r = Ripple (amplitude, greater than 10 cm)
_s = Scour (current or ice; direction noted)
_u = Unconsolidated sediment

Examples of Attribute Coding

To illustrate how these attribute codes can be used to describe remotely sensed data, the following examples are given:

Ss(s)_u = Soft unconsolidated sediment (sand) on continental shelf.
Es(s/m)_r/u = Rippled, soft, unconsolidated sediment (sand and mud) in estuary.
She_g = Hard rock outcrop (granite), on continental shelf.

Map Area Habitats

Delineated in the Drakes Bay and Vicinity map area are 19 potential marine benthic habitat types, covering 146.06 km^2 on the continental shelf ("Shelf" megahabitat). These include unconsolidated sediments (11 habitat types), mixed substrate (2 habitat types), hard substrate (4 habitat types), and anthropogenic features (2 habitat types). The predominant habitat type is soft, unconsolidated sediment, covering 135.32 km^2 (92.6 percent). Exposed hard bedrock covers 7.37 km^2 (5.0 percent); sediment-covered bedrock, which is of the mixed hard-soft induration class, covers 2.83 km^2 (1.9 percent). One shipwreck is present, although statistically insignificant; both hard and mixed anthropogenic features (unidentified, but possibly related to marine debris) cover 0.53 km^2 (0.4 percent). Rock outcrops and rubble are considered the primary habitat types for rockfish and lingcod (Cass and others, 1990; Love and others, 2002), both of which are recreationally and commercially important species. In addition, the shipwreck and other anthropogenic features may provide additional good potential habitat for rockfish.

Chapter 7. Subsurface Geology and Structure of the Drakes Bay and Vicinity Map Area and the Salt Point to Drakes Bay Region (Sheets 8 and 9)

By Janet T. Watt, Samuel Y. Johnson, and Stephen R. Hartwell

The seismic-reflection profiles presented on sheet 8 provide a third dimension, depth, to complement the surficial seafloor-mapping data already presented (sheets 1 through 7) for the Drakes Bay and Vicinity map area. These data, which are collected at several resolutions, extend to varying depths in the subsurface, depending on the purpose and mode of data acquisition. The seismic-reflection profiles (sheet 8) provide information on sediment character, distribution, and thickness, as well as potential geologic hazards, including active faults, areas prone to strong ground motion, and tsunamigenic slope failures. The information on faults provides essential input to national and state earthquake-hazard maps and assessments (for example, Petersen and others, 2008).

The maps on sheet 9 show the following interpretations, which are based on the seismic-reflection profiles on sheet 8: the thickness of the uppermost sediment unit; the depth to base of this uppermost unit; and both the local and regional distribution of faults and earthquake epicenters (data from U.S. Geological Survey and California Geological Survey, 2010; Northern California Earthquake Data Center, 2014).

Data Acquisition

Most profiles displayed on sheet 8 (figs. 1, 2, 3, 4, 6, 8, 10) were collected in 2009 on U.S. Geological Survey (USGS) cruise S–8–09–NC. The single-channel seismic-reflection data were acquired using the SIG 2Mille minisparker that used a 500-J high-voltage electrical discharge fired 1 to 4 times per second, which, at normal survey speed of 4 to 4.5 nautical miles/hour, gives a data trace every 0.5 to 2.0 m of lateral distance covered. The data were digitally recorded in standard SEG-Y 32-bit floating-point format, using Triton Subbottom Logger (SBL) software that merges seismic-reflection data with differential GPS-navigation data. After the survey, a short-window (20 ms) automatic gain control algorithm was applied to the data, along with a 160- to 1,200-Hz bandpass filter and a heave correction that uses an automatic seafloor-detection window (averaged over 30 m of lateral distance covered).

Figures 7 and 9 on sheet 8 show deep-penetration, depth-converted, multichannel seismic-reflection profiles collected in 1976 by WesternGeco on cruise W–14–76–SF. These profiles and other similar data were collected in many areas offshore of California in the 1970s and 1980s when these areas were considered a frontier for oil and gas exploration. Most of these data have been publicly released and are now archived at the U.S. Geological Survey National Archive of Marine Seismic Surveys (U.S. Geological Survey, 2009). These data were acquired using a large-volume air-gun source that has a frequency range of 3 to 40 Hz and recorded with a multichannel hydrophone streamer about 2 km long. Shot spacing was about 30 m. These data can resolve geologic features that are 20 to 30 m thick, down to subbottom depths of about 4 km.

Seismic-Reflection Imaging of the Continental Shelf

Sheet 8 shows seismic-reflection profiles in the Drakes Bay and Vicinity map area, which is characterized by predominantly seaward-dipping marine sedimentary strata of the Bodega Basin (see fig. 5 on sheet 8; see also, McCulloch, 1987), a late Tertiary shelf basin that extends from San Gregorio to Gualala (about 75 km south, and about 95 km north, of the map area, respectively). Tertiary strata overlie granitic and metamorphic basement rocks of the Salinian block, all of which have been uplifted and deformed along the Point Reyes Fault and related structures, forming the present-day Point Reyes peninsula and its adjacent continental shelf.

On seismic-reflection data, the Late Cretaceous granitic rocks are nonreflective. The overlying folded Tertiary and Pleistocene strata generally are characterized by a "ribbed" seafloor morphology that results from the variable resistance to erosion of dipping beds within the sedimentary sections. These strata are characterized by continuous, parallel to subparallel, variable amplitude, high-frequency reflections (terminology from Mitchum and others, 1977).

Surficial and shallow sediments were deposited in the last about 21,000 years during the sea-level rise that followed the Last Glacial Maximum (LGM) and the last major lowstand (Lambeck and Chappell, 2001; Peltier and Fairbanks, 2006). Sea level was about 125 m lower during the LGM, at which time the Drakes Bay and Vicinity map area was emergent. The post-LGM sea-level rise was rapid (about 9 to 11 m per thousand years) until about 7,000 years ago, when it slowed considerably to about 1 m per thousand years (Peltier and Fairbanks, 2006; Stanford and others, 2011).

The sediments deposited during the post-LGM sea-level rise (the rapid transgression and highstand) are shaded blue in the high-resolution seismic-reflection profiles on sheet 8 (figs. 1, 2, 3, 4, 6, 8, 10), and their thickness is shown on sheet 9 (Maps B, D). At the base of the post-LGM unit, distinctive sediment sequences that are characterized by channeling and various progradational patterns are present (see, for example, fig. 6 on sheet 8), representing shoreface and (or) estuarine transgressive-system-tract deposits (Catuneanu, 2006).

Geologic Structure and Recent Deformation

The northeast corner of the Drakes Bay and Vicinity Bay map area straddles the right-lateral San Andreas Fault Zone, the transform boundary between the North American and Pacific plates. Faults in the offshore part of the map area are identified on seismic-reflection profiles on the basis of the abrupt truncation or warping of reflections and (or) the juxtaposition of reflection panels that have differing seismic parameters, such as reflection presence, amplitude, frequency, geometry, continuity, and vertical sequence. The Point Reyes Fault Zone, which runs through the map area in the offshore, is a curvilinear reverse fault zone that has predominantly north-side-up motion (Hoskins and Griffiths, 1971; McCulloch, 1987; Heck and others, 1990; Stozek, 2012); this fault likely connects at depth with the west strand of the San Gregorio Fault Zone south of the map area (Ryan and others, 2008), which means that it is part of the San Andreas Fault system. The Point Reyes Fault Zone is characterized by a 5- to 11-km-wide zone of deformation in the shallow subsurface that is associated with two main fault structures, which are imaged with deep-penetration industry multichannel seismic data: the Point Reyes Fault, and also a west strand mapped offshore of the Point Reyes peninsula (see fig. 5 on sheet 8). Near the Point Reyes headland, vertical displacement of granitic basement rocks across the Point Reyes Fault is at least 1.4 km (McCulloch, 1987). Offshore of Double Point, vertical displacement on the Point Reyes Fault is difficult to assess because subsurface age constraints from nearby wells are lacking, and few offset horizons across the fault have been imaged on available seismic-reflection data. However, warping and folding of Neogene strata are clearly visible on high-resolution seismic profiles (figs. 1, 2, 3, 4 on sheet 8). The west strand of the Point Reyes Fault Zone is defined by a broad anticlinal structure, which is visible in both industry and high-resolution seismic data (see figs. 9, 10 on sheet 8). The west strand exhibits the same sense of vergence (north side up) as that of the Point Reyes Fault.

Intrastratal low-angle unconformities are common within the Tertiary and Pleistocene sections (see figs. 1, 2, 3, 4, 6, 8, 10 on sheet 8). Of particular interest is a low-angle unconformity that is imaged within the Point Reyes Syncline (see fig. 7 on sheet 8). This unconformity may represent an intrastratal unconformity within the upper Miocene and Pliocene Purisima Formation, or it may mark the boundary between the Purisima Formation and younger strata. If the folded strata above the unconformity postdate the Purisima Formation, then they record post–early Pliocene deformation within the hanging wall of the Point Reyes Fault.

A distinct unconformity (or acoustic-impedance contrast) between the upper Miocene and Pliocene Purisima Formation and younger sediments is otherwise lacking in the map area, making the distribution of upper Pliocene and Pleistocene strata difficult to ascertain from seismic-reflection data. However, lithological and paleontological data from Shell Oil Company offshore well 39–1, which was drilled into the crest of the anticline above the west strand of the Point Reyes Fault Zone (see fig. 7 on sheet 8), suggest that about 220 m of upper Pliocene and Pleistocene sediments overlie the Purisima Formation (Webster and Yenne, 1987; Heck and others, 1990) and that the upper 80 m is interpreted as being of Quaternary age (Webster and Yenne, 1987). If this is the case, then a significant amount of post–Purisima Formation strata is present on the shelf south of the Point Reyes headland that has been deformed within the Point Reyes Fault Zone. Lack of clear deformation within the post-LGM unit suggests that activity along the Point Reyes Fault Zone has diminished or slowed since about 21,000 years ago.

Map E on sheet 9 shows the regional pattern of major faults and earthquakes. Fault location is simplified and compiled from our mapping within California's State Waters (see sheet 10) and from the U.S. Geological Survey's Quaternary fault and fold database (U.S. Geological Survey and California Geological Survey, 2010). Earthquake epicenters are from the Northern California Earthquake Data Center (2014), which is maintained by the U.S. Geological Survey and the University of California, Berkeley, Seismological Laboratory; all events of magnitude 2.0 and greater for the time period 1967 through March 2014 are shown. The largest earthquake in the map area (M2.9, 4/13/1970) was located about 3.8 km southeast of the Point Reyes headland. A notable lack of microseismicity on the adjacent San Andreas Fault has occurred since the devastating great 1906 California earthquake (M7.8, 4/18/1906), thought to have nucleated on the San Andreas Fault offshore of San Francisco (see, for example, Bolt, 1968; Lomax, 2005), about 30 km south of the map area.

Thickness and Depth to Base of Uppermost Pleistocene and Holocene Deposits

Maps on sheet 9 show the thickness and the depth to base of uppermost Pleistocene and Holocene (post-LGM) deposits, both for the Drakes Bay and Vicinity map area (Maps A, B) and, to establish regional context, for a larger area (about 115 km of coast) that extends from the Salt Point area south to the southern part of the Point Reyes peninsula (Maps C, D). To make these maps, water bottom and depth to base of the LGM horizons were mapped from seismic-reflection profiles using Seisworks software. The difference between the two horizons was exported from Seisworks for every shot point as XY coordinates (UTM zone 10) and two-way travel time (TWT). The thickness of the post-LGM unit (Maps B, D) was determined by applying a sound velocity of 1,600 m/sec to the TWT, resulting in thicknesses as great as about 56 m. The thickness points were interpolated to a preliminary continuous surface, overlaid with zero-thickness bedrock outcrops (see sheet 10), and contoured following the methodology of Wong and others (2012).

Several factors required manual editing of the preliminary sediment-thickness maps to make the final product. The Gualala, Point Reyes, and San Andreas Faults disrupt the sediment sequence in the region (Maps D, E on sheet 9). The thickness data points also are dense along tracklines (about 1 m apart) and sparse between tracklines (1 km apart), resulting in contouring artifacts. To incorporate the effect of the faults, to remove irregularities from interpolation, and to reflect other geologic information and complexity, the resulting interpolated contours were modified. Contour modifications and regridding were repeated several times to produce the final regional sediment-thickness map (Wong and others, 2012). Information for the depth to base of the post-LGM unit (Maps A, C on sheet 9) was generated by adding the thickness data to water depths determined by multibeam bathymetry (see sheet 1).

The thickness of the post-LGM unit in the Drakes Bay and Vicinity map area ranges from 0 to 15 m (Map B on sheet 9), and the depth to the base of this unit ranges from 0 to 80 m (Map A on sheet 9). Mean sediment thickness for the map area is 6.0 m, and the total sediment volume is $852{\times}10^6$ m^3 (table 7–1). In general, the thickness of post-LGM sediment increases offshore where finer grained sediment is derived either locally from Drakes Estero and Estero de Limantour or from San Francisco Bay to the south (about 30 km south of the map area). The input of sand to the beaches within Drakes Bay is limited to that from local sources (cliff erosion) and from transport around the Point Reyes headland; the estimated long-term (mid- to late-1800s to 1902) rate of erosion of the beach at Limantour Spit is -0.5 m/yr (Hapke and others, 2006).

The thickest deposits are found at water depths of about 60 to 70 m where nearshore-bar deposits overlie deeper water deposits in what is referred to as the Point Reyes bar (see Map B on sheet 9). The nearshore-bar deposits are characterized by low-amplitude, prograding clinoforms, which are visible in high-resolution seismic profiles. The Point Reyes bar likely formed in the lee of the Point Reyes headland during rising sea level. These nearshore deposits overlie parallel, gently seaward-dipping reflectors (see sheet 8), which likely were deposited in deeper water (below wave base). In addition, a depocenter present within Drakes Bay (offshore of Drakes Estero and Estero de Limantour) is bounded on the south by an east-northeast-trending ridge on the Bolinas shelf, west of Point Resistance (see Map B on sheet 9). Southeast of Drakes Bay, Neogene sedimentary rocks either crop out on the seafloor or are buried by only a thin cover (mostly less than 2.5 m) of uppermost Pleistocene and Holocene sediment.

The relatively thin post-LGM sediment cover in the southeastern part of the map area is related to both active uplift and a limited sediment supply. Active uplift, which is recorded in marine terraces along the southern part of the Point Reyes peninsula, is a result of the complex interactions between the Point Reyes, San Gregorio, and San Andreas Faults (Grove and Ryan, 2007; Grove and others, 2010). The Point Reyes bar and Drakes Bay trap most of the littoral sediment supply transported from the north. In addition, west-facing coastal watersheds in this part of the Point Reyes peninsula are very small, and so much of the meager sediment that is present on the southern part of the Bolinas shelf likely is derived from local erosion of coastal bluffs or from northward transport of sediment from San Francisco Bay.

Five different “domains” of sediment thickness are recognized on the regional sediment-thickness map (Map D on sheet 9), each with distinctive geologic controls: (1) The Salt Point shelf domain, located in the far northwestern part of the region, has a mean sediment thickness of 11.7 m. The thickest sediment (20 to 25 m) is found where a pre-LGM, regressive, downlapping sediment wedge formed above a break in slope that is controlled by a contact between harder bedrock and softer, folded Pleistocene strata. Sediment thinning in this domain within the outer parts of California’s State Waters is the result of a relative lack of sediment supply from local watersheds, as well as a more distal Russian River source. (2) The Russian River delta and mud belt domain, located offshore of the Russian River, the largest sediment source on this part of the coast, has the thickest uppermost Pleistocene and Holocene sediment in the region (mean thickness, 21.1 m). The northward extension into the midshelf “mud belt” results from northward shelf-bottom currents and sediment transport (Drake and Cacchione, 1985). This domain includes a section of the San Andreas Fault Zone, which here is characterized by several releasing, right-stepping strands that bound narrow, elongate pull-apart basins; these sedimentary basins contain the greatest thickness of uppermost Pleistocene and Holocene sediment (about 56 m) in the region. (3) The Bodega Head–Tomales Point shelf domain, located between Bodega Head and the Point Reyes headland, contains the least amount of sediment in the region (mean thickness, 3.4 m). The lack of sediment primarily reflects decreased accommodation space and limited sediment supply. (4)

The Point Reyes bar domain, located west and south of the Point Reyes headland, is a local zone of increased sediment thickness (mean thickness, 14.3 m) created by bar deposition on the more protected south flank of the Point Reyes headland during rising sea level. (5) The Bolinas shelf domain, located east and southeast of the Point Reyes headland (including most of the Drakes Bay and Vicinity map area), has a thin sediment cover (mean thickness, 5.6 m), which likely reflects a limited sediment accommodation space caused by tectonic uplift (water depths in this domain within California's State Waters are less than 45 m), as well as the limited sediment supply and the high wave energy capable of reworking and transporting shelf sediment to deeper water.

Table 7–1. Area, sediment-thickness, and sediment-volume data for California's State Waters in Salt Point to Drakes Bay region (domains 1–5), as well as in Drakes Bay and Vicinity map area.

Regional sediment-thickness domains in Salt Point to Drakes Bay region			
	Area (km^2)	Mean sediment thickness (m)	Sediment volume (10^6 m^3)
Entire Salt Point to Drakes Bay region	714	9.5	6,794
(1) Salt Point shelf	90	11.7	1,054
(2) Russian River delta and mud belt	144	21.1	3,031
(3) Bodega Head–Tomales Point shelf	275	3.4	928
(4) Point Reyes bar	72	14.3	1,029
(5) Bolinas shelf	133	5.6	752
Sediment thickness in Drakes Bay and Vicinity map area			
Drakes Bay and Vicinity map area	142	6.0	852
Point Reyes bar	11	6.2	105
Bolinas shelf	131	5.6	746

Chapter 8. Geologic and Geomorphic Map of the Drakes Bay and Vicinity Map Area (Sheet 10)

By Janet T. Watt and Michael W. Manson

Geologic and Geomorphic Summary

Marine geology and geomorphology were mapped in the Drakes Bay and Vicinity map area from approximate Mean High Water (MHW) to the 3-nautical-mile limit of California's State Waters. MHW is defined at an elevation of 1.46 m above the North American Vertical Datum of 1988 (NAVD 88) (Weber and others, 2005). Offshore geologic units were delineated on the basis of integrated analyses of adjacent onshore geology with multibeam bathymetry and backscatter imagery (sheets 1, 2, 3), seafloor-sediment and rock samples (Reid and others, 2006), digital camera and video imagery (sheet 6), and high-resolution seismic-reflection profiles (sheet 8). Aerial photographs taken in multiple years were used to map the nearshore area (0 to 10 m water depth) and to link the offshore and onshore geology.

Onshore bedrock mapping is compiled from Clark and Brabb (1997), Blake and others (2000), and Wagner and Gutierrez (2010); unit ages, which are derived from these sources, reflect local stratigraphic relations. Onshore Quaternary mapping is compiled from Witter and others (2006) and Wagner and Gutierrez (2010), with some additional mapping by M.W. Manson (this report); in addition, some units are modified by M.W. Manson on the basis of analysis of 2012 lidar imagery. Traces of the San Andreas Fault are compiled from California Geological Survey (1974) and Wagner and Gutierrez (2010).

The offshore part of the map area, which includes the large embayment known as Drakes Bay, extends from the shoreline to water depths of about 40 to 60 m. The continental shelf is quite wide in this area; the shelf break is located west of the Farallon High (see fig. 1 on sheet 10), about 35 km offshore. The map area is characterized largely by a relatively flat (less than 0.8° offshore dip) bedrock platform that is overlain locally by thin veneer of Holocene sediment. Sea level has risen about 125 to 130 m during the last about 21,000 years (see, for example, Lambeck and Chappell, 2001; Peltier and Fairbanks, 2006), leading to a broadening of the continental shelf, the progressive eastward migration of the shoreline and wave-cut platform, and the associated transgressive erosion and deposition of sediment (see, for example, Catuneanu, 2006). Land-derived sediment was carried into this setting and then subjected to Pacific Ocean wave energy and strong currents before deposition or offshore transport. Shelf morphology and geology are the result of local faulting, folding, uplift, and subsidence.

The onshore part of the Drakes Bay and Vicinity map area contains part of the Point Reyes peninsula, which is located entirely west of the San Andreas Fault, the transform boundary between the Pacific and North American plates. The Point Reyes peninsula is composed of Late Cretaceous granitic rocks of the Salinian block that are overlain by Tertiary marine sedimentary rocks (Page, 1982). The Salinian block, an allochthonous (that is, out of place) tectonostratigraphic terrane, was brought north to its present-day position by right-lateral slip along the San Andreas Fault system. Since late Miocene time, the Point Reyes peninsula has been offset about 155 km along the San Gregorio and San Andreas Faults from the Monterey peninsula, where it was adjacent to Point Lobos (Greene and Clark, 1979; Clark and others, 1984; Dickinson and others, 2005).

The Point Reyes Fault Zone marks the southern boundary of the Point Reyes peninsula. It runs through the offshore part of the map area as a curvilinear reverse fault zone (Hoskins and Griffiths, 1971; McCulloch, 1987; Heck and others, 1990; Stozek, 2012) that likely connects with the west strand of the San Gregorio Fault farther south (Ryan and others, 2008). The Point Reyes Fault Zone is characterized by a 5- to 11-km-wide zone that is associated with two main fault structures: the Point Reyes Fault, and also a west strand mapped offshore of the Point Reyes peninsula (see fig. 1–1).

Offshore of the Point Reyes headland, granitic basement rocks are offset vertically (north side up) about 1.4 km on the reverse-slip Point Reyes Fault Zone (McCulloch, 1987); this uplift, combined with west-side-up offset on the San Andreas Fault Zone (Grove and Niemi, 2005), has resulted in uplift of the Point Reyes peninsula and the adjacent shelf (both the Bodega Head–Tomales Point shelf, north of the map area, and the Bolinas shelf; see sheet 9). Late Pleistocene uplift of marine terraces on the southern Point Reyes peninsula suggests active deformation of offshore structures west of the San Andreas Fault Zone (Grove and others, 2010). Offshore of Double Point, the Point Reyes Fault is associated with the warping and folding of Neogene strata, which is visible on high-resolution seismic-reflection data (see figs. 1, 2, 3, 4 on sheet 8). Although the post-Miocene slip rate on the Point Reyes Fault Zone in the map area is poorly constrained, it is estimated to be 0.3 mm/yr on the basis of vertical offset of granitic basement rocks (McCulloch, 1987; Wills and others, 2008).

Granitic basement rocks of the Salinian block are exposed onland along Inverness Ridge (unit Kgr) and west of the map area on the Point Reyes headland (mapped as unit "Kgg" in the adjacent Offshore of Point Reyes map area). Unit Kgg also is exposed offshore in the northwestern part of this (Drakes Bay and Vicinity) map area. The granitic rocks are mapped offshore on the basis of their massive, bulbous texture and extensive fracturing seen in multibeam imagery (see sheet 2), as well as their high backscatter (see sheet 3). Much of the inner shelf is underlain by Neogene marine sedimentary rocks that form the core of the Point Reyes Syncline (Weaver, 1949). These rocks include the upper Miocene Santa Margarita Formation (in the offshore, mapped as part of the undivided sedimentary rocks unit [Tu]); the middle and upper Miocene Monterey Formation (unit Tm); the upper Miocene Santa Cruz Mudstone (unit Tsc); and the upper Miocene and Pliocene Purisima Formation (unit Tp). At Millers Point, the Monterey Formation, which is exposed both onshore and on the seafloor in the nearshore, is highly fractured, making bedding planes difficult to identify. Seafloor exposures of the younger units (the Santa Cruz Mudstone [Tsc] and the Purisima Formation [Tp]) are characterized by thin to very thick bedding that commonly is gently folded and fractured, which is in contrast to the highly fractured rocks of the Monterey Formation that are visible in multibeam imagery offshore of Millers Point. Along the southeast coast of Drakes Bay, the Santa Margarita Sandstone consists of massive arkosic sandstone that rests unconformably on the Monterey Formation; in the map area, this unit is not mapped in the offshore because it consists of relatively thin (5 to 60 m thick) deposits that are difficult to identify in multibeam imagery. Strata mapped as the Monterey Formation (Tm) may also include that of the Santa Margarita Sandstone, particularly just offshore of Millers Point where no multibeam imagery exists. Seafloor outcrops mapped as the undivided sedimentary rocks unit (Tu) may include rocks of the Monterey Formation (Tm), the Santa Margarita Sandstone (mapped onland as unit Tsm), and the Santa Cruz Mudstone (Tsc). In an oil test well at Double Point, the Santa Cruz Mudstone and the underlying Santa Margarita Sandstone are more than 450 m thick (Clark and Brabb, 1997), and these units form coastal bluffs and tidal-zone exposures that extend offshore, onto the adjacent bedrock shelf. The Santa Cruz Mudstone thins markedly to the northwest, and it disappears from the section about 10 km to the northwest where the Purisima Formation unconformably overlies the Santa Margarita Sandstone. We infer that the offshore contact between the Santa Cruz Mudstone and the Purisima Formation is an angular unconformity that is visible in seismic-reflection data just southeast of the map area. This angular unconformity becomes a conformable contact to the northwest in the Drakes Bay and Vicinity map area; in addition, we suggest that this contact bends northward in the subsurface and comes onshore near U-Ranch (Galloway, 1977; Clark and Brabb, 1997). Given the lack of lithological evidence for this contact offshore of Double Point, this interpretation is speculative; an alternative interpretation is that the angular unconformity is present within the Santa Cruz Mudstone. To indicate this uncertainty, we have queried unit Tp (the Purisima Formation) in the offshore part of the map area.

Modern nearshore sediments are mostly sand (unit Qms) and a mix of sand, gravel, and cobbles (units Qmsc and Qmsd). Coarser grained sands and gravels (units Qmsc and Qmsd) are recognized primarily on the basis of bathymetry and high backscatter (sheets 1, 2, 3). Both units Qmsc and Qmsd typically have abrupt landward contacts with bedrock, and they form irregular to lenticular exposures. Contacts between units Qmsc and Qms typically are gradational.

Unit Qmsd typically is mapped as erosional lags in scour depressions (see, for example, Cacchione and others, 1984) that are bounded by relatively sharp or, less commonly, diffuse contacts with the horizontal sand sheets of unit Qms. These depressions typically are a few tens of centimeters deep and range in size from a few tens of meters to more than 1 km^2. Such scour depressions are common along this stretch of the California coast (see, for example, Cacchione and others, 1984; Hallenbeck and others, 2012; Davis and others, 2013) where offshore sandy sediment can be relatively thin (and, thus, is unable to fill the depressions) owing to lack of sediment supply from rivers and also to significant erosion and offshore transport of sediment during large northwest winter swells. Such features have been referred to as "rippled scour depressions" (see, for example, Cacchione and others, 1984) or "sorted bedforms" (see, for example, Murray and Thieler, 2004; Goff and others, 2005; Trembanis and Hume, 2011). Although the general areas in which both unit Qmsd scour depressions and surrounding Qms sand sheets are found are not likely to change substantially, the boundaries of the unit(s) likely are ephemeral, changing seasonally and during significant storm events.

Two areas of high-backscatter (see sheet 3) and rough seafloor (unit Qsr) are notable in that each includes several small (less than about 20,000 m^2), irregular "lumps" that have as much as 1 m of positive relief above the surrounding seafloor. Southeast of the Point Reyes headland, unit Qsr is mapped in water depths of between 50 and 60 m, and the orientation of the individual lumps ranges from randomly distributed to west trending. Southeast of Double Point, unit Qsr is mapped in water depths of between 30 and 40 m, and individual lumps have a more northwestward trend. Seismic-reflection data (see, for example, fig. 4 on sheet 8) reveal that this lumpy material rests on several meters of uppermost Pleistocene to Holocene sediment and, thus, is not bedrock outcrop. We interpret it as marine debris, possibly derived from the more than 60 shipwrecks that occurred offshore of the Point Reyes peninsula between 1849 and 1940 (National Park Service, 2012). It also is conceivable that this lumpy terrain consists of biological "hardgrounds" (that is, groups of fauna on the seafloor that have rigid, often calcareous, shells that exhibit high reflectivity, similar to lithified rock). Note that the video ground-truthing data that crosses unit Qsr near the Point Reyes headland (see Box A on sheet 6) was of insufficient quality to distinguish between these two alternatives.

A transition to finer grained marine sediments (unit Qmsf) is seen south of the Point Reyes headland and west of Double Point at depths of about 50 to 60 m; however, directly south and east of Drakes Estero, both backscatter data and seafloor-sediment samples (Chin and others, 1997) suggest that fine-grained sediments extend into water depths as shallow as 30 m. Unit Qmsf, which commonly is extensively bioturbated, primarily consists of mud and muddy sand. These fine-grained sediments are inferred to have been derived either locally from Drakes Estero and Estero de Limantour or from the San Francisco Bay to the south (about 30 km south of the map area) via the predominantly northwestward flow (Noble and Gelfenbaum, 1990). The relative proportions of all offshore map units are shown in table 8–1.

Table 8–1. Areas and relative proportions of offshore geologic map units in Drakes Bay and Vicinity map area.

Map Unit	Area (m^2)	Area (km^2)	Percent of total area
Marine sedimentary units			
Qms	65,460,394	65.5	42.9
Qmsc	11,622,886	11.6	7.6
Qmsf	55,942,676	55.9	36.6
Qmsd	4,438,937	4.4	2.9
Qsr	878,360	0.9	0.6
Qmsw	1,288,413	1.3	0.8
Total, sedimentary units	139,631,666	139.6	91.5
Marine bedrock and (or) shallow bedrock units			
Tp	6,009,315	6.0	3.9
Tsc	2,275,065	2.3	1.5
Tm	1,036,685	1.0	0.7
Tu	2,527,716	2.5	1.7
Kgg	1,167,705	1.2	0.8
Total, bedrock units	13,016,486	13.0	8.5
Total, Drakes Bay and Vicinity map area	152,648,152	152.6	100.0

DESCRIPTION OF MAP UNITS

OFFSHORE GEOLOGIC AND GEOMORPHIC UNITS

Qsr **Marine shelf deposits, rough seafloor (late Holocene)**—Randomly distributed to northwest-trending, irregular “lumps” (as large as 20,000 m^2) that have as much as 1 m of positive relief above seafloor; interpreted as marine debris; possibly related to either one or more shipwrecks or biological “hardgrounds”

Qms **Marine nearshore and shelf deposits (late Holocene)**—Predominantly sand (some mud); ripple marks common; found on seaward-dipping surface between the nearshore and water depths of about 65 m

Qmsc **Coarse-grained marine nearshore and shelf deposits (late Holocene)**—Predominantly coarse sand, gravel, and cobbles; found on gently seaward-dipping (less than 1°) surface in water depths typically less than about 60 m; recognized primarily on basis of high backscatter and flat relief. Extensive exposures (as much as 5 km^2) are mapped on Bodega Head–Tomales Point shelf and near mouth of Drakes Estero and Estero de Limantour where scour (caused by large waves and strong tidal currents in Drakes Bay) has winnowed away fine-grained sediments

Qmsf **Fine-grained marine shelf deposits (late Holocene)**—Predominantly mud, very fine sand, and silt; commonly bioturbated; found on gently seaward-dipping (less than 1°) surface at depths greater than about 65 to 70 m

Qmsd **Marine shelf scour depressions (late Holocene)**—Inferred to be coarse sand and possibly gravel; consists of irregular, arcuate scour depressions that vary from solitary features occupying a few hundred square meters to fields of interconnected depressions covering tens of thousands of square meters. Found as single depressions or in fields of depressions interspersed with elevated shelf sediments (units Qms and Qmsd).

Depressions typically are 15 to 50 cm deep, and they have sharp to diffuse boundaries. In map area, both backscatter data and direct camera observations (see, for example, figs. 1, 3 on sheet 4) show small intensity contrasts, suggesting that depressions are filled with sediment that is coarser than intervening elevated sandy shelf deposits; general area in which unit is found is not likely to change substantially, but boundaries of unit(s) and locations of individual depressions (and intervening flat sheets) likely are ephemeral, changing during significant storm events

Qmsw **Marine sediment wave deposits (late Holocene)**—Predominantly sand; formed by strong tidal currents that wrap around Point Reyes headland and into Drakes Bay

Tp **Purisima Formation (Pliocene and late Miocene)**—Siltstone interbedded with mudstone and sandstone; locally contains diatomite; crops out in nearshore and shelf areas southwest of Double Point and also west of U-Ranch (on Drakes Bay, about 3.5 km northwest of Point Resistance)

Tsc **Santa Cruz Mudstone (late Miocene)**—Thin- to thick-bedded marine siliceous mudstone that has carbonate concretions; crops out in nearshore and shelf areas west of Double Point

Tm **Monterey Formation (late and middle Miocene)**—Marine thin-bedded chert, porcelanite, shale, and sandstone; highly fractured offshore of Millers Point; individual beds are difficult to distinguish

Tu **Sedimentary rocks, undivided (late and middle Miocene)**—May consist of the Santa Cruz Mudstone (unit Tsc), the Santa Margarita Sandstone (mapped onland as unit Tsm), and the Monterey Formation (unit Tm)

Kgg **Point Reyes Granodiorite, porphyritic facies (Late Cretaceous)**—Contains potassium-feldspar phenocrysts that average 2 to 3 cm in length (maximum, 5 cm); seafloor outcrops appear massive, highly fractured, and bulbous

ONSHORE GEOLOGIC AND GEOMORPHIC UNITS

[Bedrock units compiled from Clark and Brabb (1997), Blake and others (2000), and Wagner and Gutierrez (2010); unit ages, which are from these sources, reflect local stratigraphic relations. Quaternary units compiled from Witter and others (2006) and Wagner and Gutierrez (2010), with some additional mapping by M.W. Manson (this report); in addition, some units modified by M.W. Manson on basis of analysis of 2012 lidar imagery]

af **Artificial fill (late Holocene)**—Engineered and (or) nonengineered

afem **Artificial fill over estuarine mud (late Holocene)**—Material deposited by humans over estuarine sediments

adf **Artificial-dam fill (late Holocene)**—Earth- or rock-fill dams, embankments and levees; constructed to impound land-locked water bodies

Qbs **Beach-sand deposits (late Holocene)**—Active beaches in coastal environment; may form veneer over bedrock platform

Qds **Dune sand (Holocene)**—Active dunes and recently stabilized dunes in coastal environments

Qe **Estuarine deposits (Holocene)**—Heterogeneous mixture of coarse and fine estuarine sediment; deposited in Drakes Estero

Qed **Estuarine-delta deposits (Holocene)**—Heterogeneous mixture of coarse and fine estuarine sediment; deposited in delta at mouths of tidally influenced coastal streams, where fresh water mixes with seawater

Qf **Alluvial fan deposits (Holocene)**—Sediment deposited by streams emanating from mountain canyons onto alluvial valley floors or alluvial plains; may include debris flow, hyper-concentrated mudflow, and braided stream deposits

Qa **Alluvial deposits, undivided (Holocene)**—Alluvium deposited in fan, terrace, or basin environments

Qls **Landslide deposits (Holocene and Pleistocene)**—Weathered rocks and soil. Internal contacts differentiate individual landslide bodies

Qmt **Marine-terrace deposits (late Pleistocene)**—Sand, gravel, and cobbles; deposited on marine-abrasion platforms and later uplifted to present-day elevations along coast

Qoc **Olema Creek Formation of Grove and others (1995) (late Pleistocene)**—Alluvial and estuarine sediments; includes sand derived from granitic rocks; interbedded with organic mud and peat

Tp **Purisima Formation (Pliocene and late Miocene)**—Siltstone interbedded with mudstone and sandstone; locally contains diatomite

Tsc **Santa Cruz Mudstone (late Miocene)**—Thin- to thick-bedded siliceous mudstone that has carbonate concretions

Tsm **Santa Margarita Sandstone (late Miocene)**—Massive arkosic sandstone

Tm **Monterey Formation (late and middle Miocene)**—Thin-bedded siliceous shale, interbedded with arkosic sandstone

Tl **Laird Sandstone of Clark and others (1984) (late and middle Miocene)**—Arkosic sandstone that contains basal granitic-boulder conglomerate

Tpr **Point Reyes Conglomerate (Paleocene)**—Sandy conglomerate, interbedded with arkosic sand

Kgr **Granodiorite and granite of Inverness Ridge (Late Cretaceous)**—Granodiorite and granite; commonly includes aplite and alaskite dikes

Kfs **Sandstone and shale of San Bruno Mountain terrane (Cretaceous)**—Sandstone and shale; part of Franciscan Complex

Acknowledgments

This publication was funded by the California Ocean Protection Council and the U.S. Geological Survey Coastal and Marine Geology Program. We thank the officers, crew, and scientific parties of the ships—R/V VenTresca, California State University, Monterey Bay, Seafloor Mapping Lab; and F/V Quicksilver, Fugro Pelagos—for their skill and professionalism in collecting the data presented in this report. We thank Bob Peters, Joe Colgan, and Scott Starratt (all USGS) for their critical reviews that greatly improved this report. We are very grateful to USGS editor Taryn Lindquist for helping us develop the templates and formats for this series of publications, and for invaluable editorial review and suggestions.

References Cited

Anderson, T.J., Cochrane, G.R., Roberts, D.A., Chezar, H., and Hatcher, G., 2007, A rapid method to characterize seabed habitats and associated macro-organisms, *in* Todd, B.J., and Greene, H.G., eds., Mapping the seafloor for habitat characterization: Geological Association of Canada Special Paper 47, p. 71–79.

Aughton, P., 2007, Francis Drake and the voyage of the Golden Hind, *in* Voyages that changed the world: London, Quercus, 208 p.

Blake, M.C., Jr., Graymer, R.W., and Jones, D.L., 2000, Geologic map and map database of parts of Marin, San Francisco, Alameda, Contra Costa, and Sonoma Counties, California: U.S. Geological Survey Miscellaneous Field Studies Map 2337, scale 1:62,500, available at http://pubs.usgs.gov/mf/2000/2337/.

Bolt, B.A., 1968, The focus of the 1906 California earthquake: Bulletin of the Seismological Society of America, v. 58, p. 457–471.

Cacchione, D.A., Drake, D.E., Grant, W.D., and Tate, G.B., 1984, Rippled scour depressions of the inner continental shelf off central California: Journal of Sedimentary Petrology, v. 54, p. 1,280–1,291.

California Department of Fish and Wildlife, 2008, California Marine Life Protection Act master plan for marine protected areas—Revised draft: California Department of Fish and Wildlife [formerly California Department of Fish and Game], available at http://www.dfg.ca.gov/mlpa/masterplan.asp.

California Geological Survey, 1974, Alquist-Priolo earthquake fault zone map of Inverness quadrangle: California Geological Survey, State of California Special Studies Zone Map, scale 1:24,000, available at http://www.quake.ca.gov/gmaps/WH/regulatorymaps.htm.

Cass, A.J., Beamish, R.J., and McFarlane, G.A., 1990, Lingcod (*Ophiodon elongatus*): Canadian Journal of Fisheries and Aquatic Sciences, Special Publication 109, 40 p.

Catuneanu, O., 2006, Principles of sequence stratigraphy: Amsterdam, Elsevier, 375 p.

Chin, J.L., Karl, H.A., and Maher, N.M., 1997, Shallow subsurface geology of the continental shelf, Gulf of the Farallones, California, and its relationship to surficial seafloor characteristics: Marine Geology, v. 137, p. 251–269, doi:10.1016/S0025-3227(96)00091-6.

Clark, J.C., and Brabb, E.E., 1997, Geology of Point Reyes National Seashore and vicinity, California—A digital database: U.S. Geological Survey Open-File Report 97–456, scale 1:48,000, available at http://pubs.usgs.gov/of/1997/of97-456/.

Clark, J.C., Brabb, E.E., Greene, H.G., and Ross, D.C., 1984, Geology of Point Reyes Peninsula and implications for San Gregorio fault history, *in* Crouch, J.K. and Bachman, S.B., eds., Tectonics and sedimentation along the California margin: Pacific Section, Society for Sedimentary Geology, v. 38, p. 67–85.

Cochrane, G.R., 2008, Video-supervised classification of sonar data for mapping seafloor habitat, *in* Reynolds, J.R., and Greene, H.G., eds., Marine habitat mapping technology for Alaska: Fairbanks, University of Alaska, Alaska Sea Grant College Program, p. 185–194, available at http://doc.nprb.org/web/research/research%20pubs/615_habitat_mapping_workshop/Individual%20Chapters%20High-Res/Ch13%20Cochrane.pdf.

Cochrane, G.R., and Lafferty, K.D., 2002, Use of acoustic classification of sidescan sonar data for mapping benthic habitat in the northern Channel Islands, California: Continental Shelf Research, v. 22, p. 683–690.

Cochrane, G.R., Conrad, J.E., Reid, J.A., Fangman, S., and Golden, N., 2005, Nearshore benthic habitat GIS for the Channel Islands National Marine Sanctuary and southern California state fisheries reserves, vol. II: U.S. Geological Survey Open-File Report 2005–1170, available at http://pubs.usgs.gov/of/2005/1170/.

Cochrane, G.R., Nasby, N.M., Reid, J.A., Waltenberger, B., and Lee, K.M., 2003, Nearshore benthic habitat GIS for the Channel Islands National Marine Sanctuary and southern California state fisheries reserves, vol. 1: U.S. Geological Survey Open-File Report 03–85, available at http://pubs.usgs.gov/of/2003/0085/.

Davis, A.C.D., Kvitek, R.G., Mueller, C.B.A., Young, M.A., Storlazzi, C.D., and Phillips, E.L., 2013, Distribution and abundance of rippled scour depressions along the California coast: Continental Shelf Research, v. 69, p. 88–100, doi:10.1016/j.csr.2013.09.010.

Dickinson, W.R., Ducea, M., Rosenberg, L.I., Greene, H.G., Graham, S.A., Clark, J.C., Weber, G.E., Kidder, S., Ernst, W.G., and Brabb, E.E., 2005, Net dextral slip, Neogene San Gregorio–Hosgri fault zone, coastal California—Geologic evidence and tectonic implications: Geological Society of America Special Paper 391, 43 p.

Drake, D.E., and Cacchione, D.A., 1985, Seasonal variation in sediment transport on the Russian River shelf, California: Continental Shelf Research, v. 4, p. 495–514, doi:10.1016/0278-4343(85)90007-X.

Fairbanks, R.G., 1989, A 17,000-year glacio-eustatic sea level record—Influence of glacial melting rates on the Younger Dryas event and deep-ocean circulation: Science, v. 342, p. 637–642.

Fleming, K., Johnston, P., Zwartz, D., Yokoyama, Y., Lambeck, K., and Chappell, J., 1998, Refining the eustatic sea-level curve since the Last Glacial Maximum using far- and intermediate-field sites: Earth and Planetary Science Letters, v. 163, p. 327–342, doi:10.1016/S0012-821X(98)00198-8.

Galloway, A.J., 1977, Geology of the Point Reyes Peninsula, Marin County, California: California Division of Mines and Geology Bulletin 202, 72 p.

Goff, J.A., Mayer, L.A., Traykovski, P., Buynevich, I., Wilkens, R., Raymond, R., Glang, G., Evans, R.L., Olson, H., and Jenkins, C., 2005, Detailed investigations of sorted bedforms, or "rippled scour depressions," within the Martha's Vineyard Coastal Observatory, Massachusetts: Continental Shelf Research, v. 25, p. 461–484, doi:10.1016/j.csr.2004.09.019.

Greene, H.G., Bizzarro, J.J., O'Connell, V.M., and Brylinsky, C.K., 2007, Construction of digital potential marine benthic habitat maps using a coded classification scheme and its application, *in* Todd, B.J., and Greene, H.G., eds., Mapping the seafloor for habitat characterization: Geological Association of Canada Special Paper 47, p. 141–155.

Greene, H.G., Bizzarro, J.J., Tilden, J.E., Lopez, H.L., and Erdey, M.D., 2005, The benefits and pitfalls of geographic information systems in marine benthic habitat mapping, *in* Wright, D.J., and Scholz, A.J., eds., Place matters: Portland, Oregon State University Press, p. 34–46.

Greene, H.G., and Clark, J.C., 1979, Neogene paleogeography of the Monterey Bay area, California, *in* Armentrout, J.M., Cole, M.R., and Ter Best, H., Jr., eds., Cenozoic paleogeography of the western United States: Pacific Coast Paleogeography Symposium 3, p. 277–296.

Greene, H.G., Yoklavich, M.M., Starr, R.M., O'Connell, V.M., Wakefield, W.W., Sullivan, D.E., McRea, J.E., and Cailliet, G.M., 1999, A classification scheme for deep seafloor habitats: Oceanologica Acta, v. 22, p. 663–678.

Grove, K., Colson, K., Binkin, M., Dull, R., and Garrison, C., 1995, Stratigraphy and structure of the Late Pleistocene Olema Creek formation, San Andreas fault zone north of San Francisco, California, *in* Sangines, E., Andersen, D., and Buising, A., eds., Recent geologic studies in the San Francisco Bay area: Society for Sedimentary Geology (SEPM), Pacific Section, Book 76, p. 55–77.

Grove, K., and Niemi, T.M., 2005, Late Quaternary deformation and slip rates in the northern San Andreas fault zone at Olema Valley, Marin County, California: Tectonophysics, v. 401, p. 231–250, doi:10.1016/j.tecto.2005.03.014.

Grove, K., and Ryan, H., 2007, Marine terrace and offshore seismic evidence for spatially and temporally varying uplift rates adjacent to the San Andreas Fault north of San Francisco, California: Geological Society of America Abstracts with Programs, v. 39, no. 6, p. 239.

Grove, K., Sklar, L.S., Scherer, A.M., Lee, G., and Davis, J., 2010, Accelerating and spatially-varying crustal uplift and its geomorphic expression, San Andreas Fault zone north of San Francisco, California: Tectonophysics, v. 495, p. 256–268, doi:10.1016/j.tecto.2010.09.034.

Hallenbeck, T.R., Kvitek, R.G., and Lindholm, J., 2012, Rippled scour depressions add ecologically significant heterogeneity to soft-bottom habitats on the continental shelf: Marine Ecology Progress Series, v. 468, p. 119–133, doi:10.3354/meps09948.

Hapke, C.J., Reid, D., Richmond, B.B., Ruggiero, P., and List, J., 2006, National assessment of shoreline change, part 3—Historical shoreline change and associated coastal land loss along sandy shorelines of the California coast: U.S. Geological Survey Open-File Report 2006–1219, 72 p., available at http://pubs.usgs.gov/of/2006/1219/.

Heck, R.G., Edwards, E.B., Kronen, J.D., Jr., and Willingham, C.R., 1990, Petroleum potential of the offshore outer Santa Cruz and Bodega basins, California, *in* Garrison, R.E., Greene, H.G., Hicks, K.R., Weber, G.E., and Wright, T.L., eds. Geology and tectonics of the central California coastal region, San Francisco to Monterey: American Association of Petroleum Geologists, Pacific Section, Bulletin GB67, p. 143–164.

Hickey, B.M., 1979, The California current system—Hypotheses and facts: Progress in Oceanography, v. 8, p. 191–279.

Hoskins, E.G., and Griffiths, J.R., 1971, Hydrocarbon potential of northern and central California offshore: American Association of Petroleum Geologists Memoir 15, p. 212–228.

Kvitek, R., Bretz, C., Cochrane, G.R., and Greene, H.G., 2006, Final report, Statewide Marine Mapping Planning Workshop, December 12–13, 2005, Seaside, Calif.: California State University, Monterey Bay, 108 p., available at http://euclase.csumb.edu/DATA_DOWNLOAD/StrategicMapgWrkshp05/MappingWorkshop12_12-13/Final_Report/CA%20Habitat%20Mapping%20Rpt.pdf.

Kvitek, R.G., Phillips, E.L., and Dartnell, P., 2012, Colored shaded-relief bathymetry, Hueneme Canyon and vicinity, California, *sheet 1 in* Johnson, S.Y., Dartnell, P., Cochrane, G.R., Golden, N.E., Phillips, E.L., Ritchie, A.C., Kvitek, R.G., Greene, H.G., Krigsman, L.M., Endris, C.A., Clahan, K.B., Sliter, R.W., Wong, F.L., Yoklavich, M.M., and Normark, W.R. (S.Y. Johnson, ed.), California State Waters Map Series—Hueneme Canyon and vicinity, California: U.S. Geological Survey Scientific Investigations Map 3225, pamphlet 41 p., 12 sheets, available at http://pubs.usgs.gov/sim/3225/.

Lambeck, K., and Chappell, J., 2001, Sea level change through the last glacial cycle: Science, v. 292, p. 679–686, doi:10.1126/science.1059549.

Lomax, A., 2005, A reanalysis of the hypocentral location and related observations for the Great 1906 California earthquake: Bulletin of the Seismological Society of America, v. 95, p. 861–877, doi:10.1785/0120040141.

Love, M.S., Yoklavich, M., Thorsteinson, L., and Butler, J., 2002, The rockfishes of the northeast Pacific: Berkeley, University of California Press, 405 p., doi:10.5860/CHOICE.40-3403.

Madden, C.J., Goodin, K.L., Allee, R., Finkbeiner, M., and Bamford, D.E., 2008, Draft Coastal and Marine Ecological Classification Standard: National Oceanic and Atmospheric Administration (NOAA) and NatureServe, v. III, 77 p.

McCulloch, D.S., 1987, Regional geology and hydrocarbon potential of offshore Central California, *in* Scholl, D.W., Grantz, A., and Vedder, J.G., eds., Geology and resource potential of the continental margin of western North America and adjacent ocean basins—Beaufort Sea to Baja California: Circum-Pacific Council for Energy and Mineral Resources, Earth Science Series, v. 6, p. 353–401.

Mitchum, R.M., Jr., Vail, P.R., and Sangree, J.B., 1977, Seismic stratigraphy and global changes of sea level, part 6—Stratigraphic interpretation of seismic reflection patterns in depositional sequences, *in* Payton, C.E., ed., Seismic stratigraphy—Applications to hydrocarbon exploration: Tulsa, Okla., American Association of Petroleum Geologists, p. 117–133.

Murray, B., and Thieler, E.R., 2004, A new hypothesis and exploratory model for the formation of large-scale inner-shelf sediment sorting and “rippled scour depressions”: Continental Shelf Research, v. 24, no. 3, p. 295–315, doi:10.1016/j.csr.2003.11.001.

National Park Service, 2012, Shipwrecks on the Point Reyes Peninsula 1849–1940, *in* Shipwrecks at Point Reyes: National Park Service Web site, available at http://www.nps.gov/pore/historyculture/upload/map_shipwrecks.pdf.

Noble, M.A., 2001, Current patterns over the Continental Shelf and Slope, *in* Karl, H.A., Chin, J.L., Ueber, E., Stauffer, P.H., and Hendley, J.W., II, eds., Beyond the Golden Gate—Oceanography, geology, biology, and environmental issues in the Gulf of the Farallones: U.S. Geological Survey Circular 1198, p. 67–89, available at http://pubs.usgs.gov/circ/c1198/.

Noble, M.A., and Gelfenbaum, G., 1990, A pilot study of currents and suspended sediment in the Gulf of the Farallones: U.S. Geological Survey Open-File Report 90–476, 30 p.

Northern California Earthquake Data Center, 2014, Northern California earthquake catalog: Northern California Earthquake Data Center database, accessed April 5, 2014, at http://www.ncedc.org/ncsn/.

Page, B.M., 1982, Migration of Salinian composite block, California, and disappearance of fragments: American Journal of Science, v. 282, p. 1,694–1,734, doi:10.2475/ajs.282.10.1694.

Patsch, K., and Griggs, G., 2007, Development of sand budgets for California’s major littoral cells—Report prepared for the California Coastal Sediment Management Workgroup: California Department of Boating and Waterways, January 2006, 115 p.

Peltier, W.R., and Fairbanks, R.G., 2006, Global glacial ice volume and Last Glacial Maximum duration from an extended Barbados sea level record: Quaternary Science Reviews, v. 25, p. 3,322–3,337, doi:10.1016/j.quascirev.2006.04.010.

Petersen, M.D., Frankel, A.D., Harmsen, S.C., Mueller, C.S., Haller, K.M., Wheeler, R.L., Wesson, R.L., Zeng, Y., Boyd, O.S., Perkins, D.M., Luco, N., Field, E.H., Wills, C.J., and Rukstales, K.S., 2008, Documentation for the 2008 update of the United States National Seismic Hazard Maps: U.S. Geological Survey Open-File Report 2008–1128, 61 p., available at http://pubs.usgs.gov/of/2008/1128/.

Phillips, E.L., Storlazzi, C.D., Dartnell, P. and Edwards, B.D., 2007, Exploring rippled scour depressions offshore Huntington Beach, California: Coastal Sediments 2007, v. 3, p. 1,851–1,864.

Reid, J.A., Reid, J.M., Jenkins, C.J., Zimmerman, M., Williams, S.J., and Field, M.E., 2006, usSEABED—Pacific Coast (California, Oregon, Washington) offshore surficial-sediment data release: U.S. Geological Survey Data Series 182, available at http://pubs.usgs.gov/ds/2006/182/.

Ryan, H.F., Parsons, T., and Sliter, R.W., 2008, Vertical tectonic deformation associated with the San Andreas fault zone offshore of San Francisco, California: Tectonophysics, v. 457, p. 209–223, doi:10.1016/j.tecto.2008.06.011.

Stanford, J.D., Hemingway, R., Rohling, E.J., Challenor, P.G., Medina-Elizalde, M., and Lester, A.J., 2011, Sea-level probability for the last deglaciation—A statistical analysis of far-field records: Global and Planetary Change, v. 79, p. 193–203, doi:10.1016/j.gloplacha.2010.11.002.

Stozek, B.A., 2012, Geophysical evidence for Quaternary deformation within the offshore San Andreas fault system, northern California: San Francisco, Calif., San Francisco State University, M.S. thesis, 141 p.

Tissot, B.N., Yoklavich, M.M., Love, M.S., York, K., and Amend, M., 2006, Benthic invertebrates that form habitat on deep banks off southern California, with special reference to deep sea coral: Fishery Bulletin, v. 104, p. 167–181.

Trembanis, A.C., and Hume, T.M., 2011, Sorted bedforms on the inner shelf off northeastern New Zealand—Spatiotemporal relationships and potential paleo-environmental implications: Geo-Marine Letters, v. 31, p. 203–214, doi:10.1007/s00367-010-0225-8.

U.S. Geological Survey, 2009, National Archive of Marine Seismic Surveys: U.S. Geological Survey database, available at http://walrus.wr.usgs.gov/NAMSS/.

U.S. Geological Survey and California Geological Survey, 2010, Quaternary fault and fold database of the United States: U.S. Geological Survey database, accessed April 5, 2014, at http://earthquake.usgs.gov/hazards/qfaults/.

Wagner, D.L., and Gutierrez, C.I., 2010, Preliminary geologic map of the Napa 30′ × 60′ quadrangle, California: California Geological Survey, scale 1:100,000, available at http://www.conservation.ca.gov/cgs/rghm/rgm/Pages/preliminary_geologic_maps_1page.aspx.

Weaver, C.E., 1949, Geology of the Coast Ranges immediately north of San Francisco Bay region, California: Geological Society of America Memoir 35.

Weber, K.M., List, J.H., and Morgan, K.L., 2005, An operational Mean High Water datum for determination of shoreline position from topographic lidar data: U.S. Geological Survey Open-File Report 2005–1027, available at http://pubs.usgs.gov/of/2005/1027/.

Webster, F., and Yenne, K.A., 1987, Northern and central California lease sale/May 14, 1963: U.S. Department of the Interior Mineral Management Service, Pacific OCS Region, OCS Report MMS 87–0108, 48 p.

Wentworth, C.K., 1922, A scale of grade and class terms for clastic sediments: Journal of Geology, v. 30, p. 377–392.

Wills, C.J., Weldon, R.J., II, and Bryant, W.A., 2008, Appendix A—California fault parameters for the National Seismic Hazard Maps and Working Group on California Earthquake Probabilities 2007, *in* The Uniform California Earthquake Rupture Forecast, version 2 (UCERF 2): U.S. Geological Survey Open-File Report 2007–1437A and California Geological Survey Special Report 203A, 48 p., available at http://pubs.usgs.gov/of/2007/1437/a/.

Witter, R.C., Knudsen, K.L., Sowers, J.M., Wentworth, C.M., Koehler, R.D., Randolph, C.E., Brooks, S.K., and Gans, K.D., 2006, Maps of Quaternary deposits and liquefaction susceptibility in the central San Francisco Bay region, California: U.S. Geological Survey Open-File Report 2006–1037, scale 1:24,000, available at http://pubs.usgs.gov/of/2006/1037/.

Wong, F.L., Phillips, E.L., Johnson, S.Y, and Sliter, R.W., 2012, Modeling of depth to base of Last Glacial Maximum and seafloor sediment thickness for the California State Waters Map Series, eastern Santa Barbara Channel, California: U.S. Geological Survey Open-File Report 2012–1161, 16 p., available at http://pubs.usgs.gov/of/2012/1161/.

Wright, D.J., Pendleton, M., Boulware, J., Walbridge, S., Gerlt, B., Eslinger, D., Sampson, D., and Huntley, E., 2012, ArcGIS Benthic Terrain Modeler (BTM), v. 3.0: Environmental Systems Research Institute and NOAA Coastal Services Center, Massachusetts Office of Coastal Zone Management, accessed February 1, 2013, at http://esriurl.com/5754.